ARCHIVIO ISTITUZIONALE
DELLA RICERCA

Alma Mater Studiorum Università di Bologna
Archivio istituzionale della ricerca

PL10 DEAD-Box Protein is Expressed during Germ Cell Differentiation in the Reptile Podarcis sicula (Family Lacertidae)

This is the final peer-reviewed author's accepted manuscript (postprint) of the following publication:

Published Version:
Milani, L., Pecci, A., Cifaldi, C., Maurizii, M.G. (2017). PL10 DEAD-Box Protein is Expressed during Germ Cell Differentiation in the Reptile Podarcis sicula (Family Lacertidae). JOURNAL OF EXPERIMENTAL ZOOLOGY. PART B, MOLECULAR AND DEVELOPMENTAL EVOLUTION, 328(5), 433-448 [10.1002/jez.b.22744].

Availability:
This version is available at: https://hdl.handle.net/11585/607212 since: 2018-09-21

Published:
DOI: http://doi.org/10.1002/jez.b.22744

Terms of use:

Some rights reserved. The terms and conditions for the reuse of this version of the manuscript are specified in the publishing policy. For all terms of use and more information see the publisher's website.

This item was downloaded from IRIS Università di Bologna (https://cris.unibo.it/).
When citing, please refer to the published version.

(Article begins on next page)

08 July 2024

This is the peer reviewed version of the following article:

Milani L, Pecci A, Cifaldi C, Maurizii MG. 2017. PL10 DEAD-box protein is expressed during germ cell differentiation in the reptile Podarcis sicula (Family Lacertidae). *J Exp Zool (Mol Dev Evol)*. 328B:433–448

which has been published in final form at https://doi.org/10.1002/jez.b.22744.

This article may be used for non-commercial purposes in accordance with Wiley Terms and Conditions for Use of Self-Archived Versions.

PL10 DEAD-box protein is expressed during germ cell differentiation in the reptile *Podarcis sicula* (Family Lacertidae)

Liliana Milani*, Andrea Pecci, Carmine Cifaldi, and Maria Gabriella Maurizii

Department of Scienze Biologiche, Geologiche ed Ambientali, University of Bologna, Via Selmi 3, 40126, Bologna, Italy.

* corresponding author:
orcid ID: 0000-0001-5052-2075
liliana.milani@unibo.it
+39 051 2094220
+39 051 2094286

Running title: PL10 expression in the germ line of *Podarcis sicula*.

ABSTRACT

Among genes involved in the regulation of germ cell differentiation, those of DDX4/Vasa- and the Ded1/DDX3-subfamilies encode for DEAD-box ATP-dependent RNA helicases, proteins involved in many mechanisms related to RNA processing. For the first time in reptiles, using specific antibodies, we analyzed at confocal microscopy the localization pattern of a Ded1/DDX3-subfamily member in testis and ovary of *Podarcis sicula* (Ps-PL10) during the reproductive cycle. In testis, Ps-PL10 is expressed in the cytoplasm of spermatocytes, while it is not detected in spermatogonia. Differently from Ps-VASA, in round spermatids Ps-PL10 is not segregated in the chromatoid body but it accumulates in the cytoplasm of residual bodies, and mature spermatozoa result unstained. These observations suggest that in males Ps-PL10: 1) is involved in spermatogenesis, and 2) is then eliminated with residual bodies. In the ovary, Ps-PL10 is present with granules in the cytoplasm of early meiotic cells of the germinal bed (GB), while it is not present in oogonia and somatic cells of the GB stroma. In follicular cells of ovarian follicles, Ps-PL10 expression starts after their fusion with the oocyte. Numerous Ps-PL10 spots are visible in pyriform (nurse-like) cells concomitantly with the protein accumulation in the cytoplasm of differentiating oocyte. In pyriform cells, Ps-PL10 spots are present in the cytoplasm and nuclei, as observed for Ps-VASA, and in the nucleoli, suggesting for Ps-PL10 a role in rRNA processing, in the transport of molecules from the nucleus to cytoplasm and from nourse cells to the oocyte.

Keywords: Ded1/DDX3, DDX4/Vasa, gametogenesis, testis, ovary, residual body.

INTRODUCTION

In recent years, a number of "germ line factors" driving germ cell differentiation in both sexes have been identified in several species. Among these factors, the genes of DDX4/Vasa and Ded1/DDX3 subfamilies have been investigated in several invertebrates and vertebrates (Raz, 2000; Leclère et al., 2012; Sharma and Jankowsky, 2014; Kozin and Kostyuchenko, 2015; Siebert et al., 2015; Fierro-Constaín et al., 2017). These genes encode for DEAD-box ATP-dependent RNA helicases (Linder et al., '89), proteins found in all eukaryotes and most prokaryotes (e.g. Schmid and Linder, '92; Fujiwara et al., '94; Komiya et al., '94; Fabioux et al., 2004; Zhou et al., 2010). The DEAD-box family proteins are characterized by nine conserved motifs, such as the D-E-A-D (Asp-Glu-Ala-Asp) box from which the family is named after, and are involved in many processes related to RNA, ranging from its synthesis to splicing, translation, degradation, stability and nucleocytoplasmic transport (Linder and Jankowsky, 2011; Linder and Fuller-Pace, 2013, 2015).

The DEAD-box proteins are divided into subfamilies according to their sequence and function. DDX4/Vasa, Ded1/DDX3, and p68/DDX5 are closely-related subfamilies whose homologs form highly supported and distinct clusters in phylogenetic analysis (Wang et al., 2012).

p68/DDX5 proteins are among the first DEAD-box for which RNA helicase activity was demonstrated *in vitro* (Ford et al., '88; Hirling et al., '89). These proteins are expressed in meiotic testicular cells but also in various other tissues (Hirling et al., '89; Lemaire and Heinlein, '93).

DDX4/Vasa proteins are expressed in both male and female germ cells (Lasko and Ashburner, '88) and are essential in gametogenesis and in of germ cell specification during embryogenesis (Raz, 2000). Nonetheless, in some animals, DDX4/Vasa proteins are also

expressed in stem cells of diverse origin, in which they contribute to cell cycle and developmental regulation (Leclère et al., 2012; Kozin and Kostyuchenko, 2015; Siebert et al., 2015; Yajima and Wessel, 2015; Fierro-Constaín et al., 2017). In other animals, their expression appears to be restricted to the germ cell lineage (Zhou et al., 2010).
Ded1/DDX3 members are present in a wide range of eukaryotes (Sharma and Jankowsky, 2014); table 1 reports data about animals, the object of this study. In invertebrates and non-mammal vertebrates, Ded1/DDX3 genes are often named *pl10*. In invertebrates, as for example *Hydra*, planarians, and *Drosophila*, they are important for spermatogenesis and differentiation (Mochizuki et al., 2001; Solana and Romero 2009; Kotov et al., 2016). Among vertebrates, Ded1/DDX3 genes are deeply studied in mammals. The mouse, for example, has three Ded1/DDX3 genes (Gee and Conboy, '94; Sowden et al., '95). An autosomal form (PL10) is expressed in testicular tissues at the pachytene stage of male meiosis (Leroy et al., '89; Inoue et al., 2016) with a possible role in translational regulation (Chuang et al., '97). Instead, the human genome contains two homologs of the Ded1/DDX3 subfamily, with an Y-linked form translated only in testes, especially in spermatogonia (Foresta et al., 2000; Ditton et al., 2004). In non-mammal animals, as well as in non-eutherian mammals, *pl10* is, with few exceptions (see Fierro-Constaín et al., 2017), the sole member of the subfamily (Chang and Liu, 2010). Several detailed, recent studies documented its localization pattern in animals such as sponges and cnidarians, while the study of its localization in vertebrates is limited (see Table 1). In zebrafish, RNA *in situ* hybridisation revealed that the *pl10*-homologous gene (*pl10a*) is highly transcribed in germ cells (Olsen et al., '97). *Xenopus laevis pl10* (*an3*) has been localized as transcript predominantly to the animal hemisphere of oocytes (Gururajan et al. '94; Gururajan and Weeks, '97), as also documented for one of the three Ded1/DDX3 of the mouse (Sowden et al., '95). Specifically, during *X. laevis* oogenesis, An3 protein can be found both in the cytoplasm, in the nucleus

and in the nucleoli (Gururajan et al., '94).

There are no available data regarding Ded1/DDX3 (PL10) localization and expression in reptiles. Recently, a DEAD-box protein belonging to the DDX4/Vasa subfamily (Ps-VASA) was specifically localized in both female and male germ cells of the lizard *Podarcis sicula* (Maurizii et al., 2009; Milani and Maurizii, 2014, 2015).

The aim of the present work was to characterize a Ded1/DDX3 protein for the first time in a reptile and to document its expression during the differentiation process of germ cells, comparing its localization with that of VASA. Firstly, we sequenced a portion of *P. sicula pl10* homologous gene (*Ps-pl10*), and we developed two specific antibodies on the inferred amino acid sequence (anti-Ps-PL10). Then, we utilized anti-Ps-PL10 to analyse, at confocal microscopy, the localization pattern of the protein during gametogenesis. In particular, Ps-PL10 expression was analyzed during spermatogenesis in the adult male, in all phases of the reproductive cycle, in the juvenile male (when seminiferous tubules are forming), and during early oogenesis in adult female, both in hibernating and metabolically active lizards. The present work adds insights into reptiles broadening the knowledge about Ded1/DDX3 protein expression, moreover, since non-model organisms are important in the field of comparative biology and evolutionary developmental biology, we think that filling this gap will be useful to reach a comprehensive overview on the topic.

MATERIALS AND METHODS

Experimental animals

Sexually mature specimens of *P. sicula* Raf. (15 females and 15 males), collected in the neighbourhoods of Naples (Italy), were used in this study.

In particular, to analyze the expression pattern of Ps-PL10 in adult testis in each phases of the reproductive cycle, we sacrificed animals in different periods of the year: in the spring (May),

during full gonadic activity with spermiation, in the summer (end of July) during regression, and in November, during slow autumnal recrudescence without spermiation. Moreover, in November, two *P. sicula* young males were used to study testes in which the germ cells inside the epithelium of the seminiferous tubules were forming.

To analyse the expression pattern of Ps-PL10 in adult ovaries, we used metabolically active (spring-summer) and hibernating (winter) lizards. The animals were kept under seasonal environmental conditions with respect to temperature and light and were fed with insects. All procedures were in accordance with the guidelines of the European Communities Council Directive (86/609/CEE), the current Italian legislation for the use and care of animals, and conformed to the guidelines of the US National Institutes of Health.

Sequencing and gene characterization

Total RNA of gonads was isolated using TRIzol® RNA Isolation Reagents (Life Technologies); SuperScript™ First-Strand Synthesis System for RT-PCR was used to obtain cDNA. Given the absence of *P. sicula pl10* gene in database, we used primers already available in our Lab and constructed on conserved regions of other RNA helicases. We used two primer pairs: T1-forward -ATGGCNTGYGCNCARACNGG- and T1-reverse-CATNCGRTCNGCYCTATCNAGNAC- (Tsunekawa et al., 2000), and VAS_A-ATGGCNTGYGCNCARACNGG- and VAS_E-GGCATRTCRTARTTDATNACRTG- (Fabioux et al., 2004). Sequencing was performed at Macrogen Inc. (Seoul, South Korea). Nucleotide sequences were assembled and aligned with MEGA7 (Kumar et al., 2016). The obtained sequences were translated and the amino acid sequences analysed, using the online BLAST at NCBI, to assess their similarity with other DEAD-box proteins in GenBank. We aligned the obtained protein with orthologous sequences downloaded from UniProt. Orthology was assessed with OrthoMCL (www.orthomcl.org; Fischer et al., 2011). InterPro

(http://www.ebi.ac.uk/interpro/; Mitchell et al., 2015) was used to search for conserved protein domains. We also performed a phylogenetic analysis based on the Neighbor Joining (NJ) and Maximum Likelihood (ML) methods (Mega 7; 1,000 bootstrap replicates) including proteins belonging to DDX4/Vasa, Ded1/DDX3, and p68/DDX5 subfamilies.

Antibody production

The amino acid sequence obtained for *P. sicula* PL10 (Ps-PL10) allowed us to choose two peptides with "good antigenicity", "good solubility" and "good epitope prediction" (according to the computational analyses performed by Davids Biotechnology) that were used for rabbit immunization. Two specific antibodies were generated against the two peptides YEEARKFAYRSKVRPC and DALRAMKENGRYGRRKQY (anti-Ps-PL10-YEE and anti-Ps-PL10-DAL, respectively). The obtained antibodies were tested for immunoreactivity by ELISA with the corresponding immunogen peptide and were later purified by affinity chromatography. The immunization protocol, the immunoreactivity test, and the affinity purification from rabbit serum were carried out by a biotechnology company (Davids Biotechnologie, Regensburg, Germany).

SDS-PAGE and Western blot analyses

Ovaries and testes were homogenized, using an Ultra Turrax T25 (Janke & Kunkel IKA-labortechnik), in a buffer containing 10 mM Tris–HCl, pH 7.5, 1 mM ethylene glycol-bis(2-aminoethyl ether)-N,N,N',N'-tetraacetic acid (EGTA) and in the presence of the following protease inhibitors: 1 mM PMSF and 2× protease inhibitor cocktail tablets (Complete Mini of Roche). The homogenate was centrifuged at 4°C at 7,500 rcf for 10-20 min, depending on the clearness of the supernatant. Supernatant proteins were quantified using the Lowry method (Lowry et al., '51). Extracts (30-40 μg of total proteins) were utilized for SDS-PAGE and

immunoblotting as previously described in Milani and Maurizii (2015). Membranes were incubated with rabbit anti-Ps-PL10-YEE and anti-Ps-PL10-DAL, diluted 1:1,000 with 0.1% Tween 20 (Tw) (Sigma) in Tris Buffered Saline solution (TBS: 200 mM Trizma base; 137 mM NaCl), namely TBS-0.1%Tw, overnight at 4°C, plus 1 h 15 min at room temperature (RT). After rinsing, membranes were incubated with goat anti-rabbit secondary antibody, conjugated with horseradish peroxidase (Santa Cruz Biotechnology Inc., Santa Cruz, CA, USA) diluted 1:5,000 in TBS-0.1% Tw for 1 h and 15 min at RT. After washes, membranes were treated with ECL Western Blotting Detection Reagents (Santa Cruz Biotechnology Inc.) and exposed to Hyperfilm ECL (GE Healthcare). As negative control, the primary antibody was preincubated for 1 h at RT with a 10-fold molar excess (w/v) of the peptide against which it was raised.

Confocal microscopy analyses

Tissue processing

Ovaries and testes were rapidly removed and fixed with 3.7% paraformaldehyde plus 0.25% or 0.5% glutaraldehyde in a buffer containing 80 mM KPIPES, 1 mM $MgCl_2$, 5 mM ethylene glycol bis(2-aminoethyl ether)-N,N,N′,N′-tetraacetic acid (EGTA) and 0.2% Triton X-100 (T), pH 7.2, for 4-6 h (glutaraldehyde concentration and the fixation time depends on gonad size) at RT. Ovaries for microtubules staining were fixed as previously reported (Milani and Maurizii, 2015). Fixed ovaries and testes were washed with phosphate-buffered saline (PBS) (128 mM NaCl, 2 mM KCl, 8 mM Na_2HPO_4, 2 mM KH_2PO_4), pH 7.2, for 1 h, and embedded in 6% agar. Sections of 80-100 µm thickness, obtained using a Lancer Vibratome Series 1000, were post-fixed with increasing concentrations of methanol (50-100%) and processed as free-floating sections for immunofluorescence. Non-specific protein-binding sites were blocked in TBS supplemented with 0.1% Triton (T) containing 1% bovine

serum albumin (BSA), 10% normal goat serum (NGS) (both from Sigma), pH 7.4 for 1 h and 30 min at RT.

PL10 immunostaining

As primary antibodies we used anti-Ps-PL10-YEE and anti-Ps-PL10-DAL diluted 1:7,000 and 1:5,000, respectively, with 1% NGS, 1% BSA in TBS-0.1% T, pH 7.4, and incubated at 4°C for about 60 h. After washing, sections were incubated with a goat anti-rabbit polyclonal antibody conjugated with Alexa Fluor® 488 (Jackson ImmunoResearch Laboratories, Inc.), diluted 1:400 with 1% NGS and 1% BSA in TBS-0.1%T for 24 h at 4°C, 1 h at RT, and then washed.

α-tubulin immunostaining

Ovary sections, after digestion for 17 min at RT with 0.01% Pronase E (Merck) in PBS, pH 7.2, followed washes in PBS, were incubated with DM1A, a monoclonal anti-α-tubulin (Sigma), diluted 1:500 with TBS-0.1% T containing 2% BSA, for 60 h at 4°C and then washed extensively for 24–32 h. Finally, sections were incubated for 32 h at 4°C with anti-mouse secondary antibody Alexa-Fluor 488® (1:400; Jackson Immunoresearch) and then washed.

All the sections, independently on the antibody used, were also stained with a nuclear dye, 1 mM TO-PRO 3 iodide (Molecular Probes) in PBS, pH 7.2, for 10 min and, after washing, the sections were placed in drops of TBS on microscope slides. Then the TBS was replaced with 2.5% DABCO [1,4-diazabicyclo[2.2.2]octane) (Sigma), 50 mmol Tris, pH 8, and 90% glycerol], and the slides covered by coverslips and sealed with nail polish.

Controls were performed using sections treated with NGS without primary antibodies before being incubated with the secondary antibody.

Sections were examined with Leica TCS SL SP2 and Leica TCS SP8 X confocal laser scanning microscopes, using Leica confocal software. Images were analysed with Fiji (Schindelin et al., 2012).

RESULTS

Sequence analyses

Sequence similarity detected using BLAST indicated that the sequences obtained using VAS_AE and T1 primer pairs belonged to Ded1/DDX3 family. For this reason, we aligned and merged the two sequences, obtaining a longer portion of the newly characterized *P. sicula pl10* gene (Ps-*pl10* partial sequence, GenBank accession number KU898904; protein sequence Ps-PL10, 284 amino acids, AA). InterPro highlighted the presence of characteristic domains of the DEAD-box proteins: AA 2-171 DEAD-box helicase domain (Pfam), and AA 194-284 Helicase C terminal domain (PROSITE) (Fig. 1). The trees showed that Ps-PL10 sequence clustered with proteins of the Ded1/DDX3 subfamily (Fig. 2; sequence alignment in Supplementary Material 1). The alignment of Ps-PL10 and orthologs from a sample of species shows conserved regions in the protein domains (Fig. 1).

Antibody immunoreactivity and specificity

We carried out Western blots of *P. sicula* gonadic extracts to test the immunoreactivity of the newly produced anti-Ps-PL10 antibodies (antigenic peptides highlighted in Fig. 1). In ovary and testis extracts, anti-Ps-PL10-YEE and anti-Ps-PL10-DAL detected one band (72 kDa) (Fig. 3) or two bands (70 and 72 kDa) (Supplementary Material 2). Western blot in which the primary antibody was preincubated with a 10-fold molar excess (w/v) of the peptide against which it was produced showed a strong attenuation of the 70/72 kDa bands, supporting antibody specificity (Fig. 3; Supplementary Material 2).

Confocal microscopy

PL10 expression during spermatogenesis

Ps-PL10 immunolocalization was analysed in each phase of the reproductive circannual cycle of adult testis of *P. sicula* and also in immature testis (Figs. 4-7 using anti-Ps-PL10-YEE; Supplementary Material 2 using anti-Ps-PL10-DAL).

Full gonadic activity

In the seminiferous tubule in the spring, the marginal region of the lumen in cross section shows many spermatozoa (Fig. 4A,B); the wall of the seminiferous epithelium shows different generations of germ cells: spermatogonia, close to the basal membrane, and, in succession, a large population of spermatocytes I and II; many stages of spermatids in differentiation (elongation and maturation) are present in the apical region of the tubule (Fig. 4A). In this phase, Ps-PL10 is present in the cytoplasm of both spermatocytes I and II with many small and dispersed positive granules and some bigger immunospots representing aggregation of PL10 protein; no staining is observable in spermatogonia and Sertoli cells (Fig. 4C). A strong Ps-PL10 staining is evident in the cytoplasm of late spermatids, at the final stages of differentiation, just before spermiation, localized close to the tubule lumen (Fig. 4A,D). Spermatozoa released in the tubule lumen are unstained (Fig. 4B).

Regression of gonadic activity in the summer

In late July, seminiferous tubules in cross section show few unstained mature spermatozoa in the lumen (Fig. 5A). In this phase, a stronger Ps-PL10 immunostaining is visible in the apical region, in particular in the lumen (Fig. 5A,B), if compared to what observed during full gonadic activity. A magnification of this region shows immunostained masses and

immunostained cells that fill the lumen (Fig. 5C). In the wall of the seminiferous tubule, spermatogonia, that in this phase represent the majority of the germ cells, are unstained and some of them are in proliferation, while spermatocytes show small positive granules and some bigger immunospots in their cytoplasm (Fig. 5A).

Slow autumnal recrudescence

In mid-late November, when animals start semi-hibernating (winter stasis), the epithelium of seminiferous tubules increases in thickness and each stage of differentiating germ cells is visible (Fig. 6A), with Ps-PL10 expression present only in meiotic cells (spermatocytes I and II) (Fig. 6B). In the small lumen, few unstained spermatozoa are present (Fig. 6A).

In immature testes, when seminiferous tubules are forming, a low number of spermatogonia and spermatocytes is present in the wall (Fig. 7A). Ps-PL10 is detected in meiotic cells in the central region of the tubule (Fig. 7B), whereas spermatogonia, localized near the basal lamina, result unstained.

PL10 expression during early oogenesis

The distribution of Ps-PL10 was analysed in adult ovaries from metabolically active and hibernating animals (Figs. 8, 9 using anti-Ps-PL10-YEE; Supplementary Material 2 using anti-Ps-PL10-DAL), in particular: in the germinal bed (GB), where germ cells begin their differentiation, and in ovarian follicles during the most of the pre-vitellogenic oocyte growth, when the differentiation of follicular cells takes place.

Germinal bed of metabolically active animals

In the spring-summer, the GB shows some germ cells organized in clusters and others, in different differentiation stages, dispersed among the somatic cells of the stroma (Fig. 8A). In

P. sicula, as in other lizards, and unlike mammals and birds, the GB, a small region located at the dorsal surface of the ovary, is responsible for the continuous renewal of germ cells during the reproductive lifespan (Filosa, '73; Jones et al., '82). The GB consists of dividing oogonia, early meiotic naked oocytes and primordial follicles immersed in a stroma of somatic cells (Filosa, '73; Jones et al., '82). Oogonia and early meiotic oocytes (up to zygo-pachytene stage of meiotic prophase) are organized in clusters constituted by synchronized cells connected by intercellular bridges and bounded by stroma cells. This syncytial organization of the clustered germ cells disappears at the stage of early diplotene, leading to isolated oocytes surrounded by stroma cells (Filosa and Taddei, '76a,b). Such clusters can contain one or the other of two types of germ cells characterized by a roundish nucleus: those with compact chromatin are likely oogonia, those with dispersed chromatin are likely very early meiotic oocytes (Fig. 8A). No Ps-PL10 staining is detectable in oogonia (Fig. 8A). Ps-PL10 expression started in early meiotic oocytes with many granules and few, bigger immunospots in their cytoplasm (Fig. 8B). The somatic cells of the GB stroma, recognizable for their elongated nucleus, are Ps-PL10-unstained (Fig. 8A,B).

Pre-vitellogenic ovarian follicles of metabolically active animals

Oocytes surrounded by a monolayer of follicle cells are released from the GB and represent early follicles (Andreuccetti et al., '78) (Fig. 8C). These oocytes show in the cytoplasm bigger Ps-PL10-stained spots (Fig. 8C-E) than those observed in early meiotic oocytes (Fig. 8B). Stained spots appear concentrated in the perinuclear region (Fig. 8C-E). No Ps-PL10 staining is visible in the cytoplasm of the follicular cells surrounding the oocytes (Fig. 8C-E). In the follicular epithelium, starting from ovarian follicles of about 100 μm in diameter, some follicular cells enlarge (becoming intermediate cells) and later, in larger ovarian follicles (Fig. 9C), differentiate into pyriform cells (Filosa et al., '79). With anti-α-tubulin staining the

intercellular bridges between these cells and the oocyte are well evident (Fig. 9A,C). Ps-PL10 expression is present in intermediate cells with few immunospots in their cytoplasm (Fig. 8C and Fig. 9B), in the nucleus (Fig. 9D), and also in the nucleolus (Fig. 9B), in which the staining is visible only in projection of more optical sections. Ps-PL10 was detected as a larger number of spots in the well differentiated pyriform cells of ovarian follicles of about 800-1,000 μm in diameter (Fig. 9C) with numerous spots present in the cytoplasm and in the nucleus (Fig. 9D,E) (for nucleolar staining in this stage see Supplementary Material 2). The number of Ps-PL10-stained spots increase in the oocyte cytoplasm with its size (Fig. 8F and Fig. 9D). All small somatic follicular cells result unstained (Fig. 9B,D,E).

Hibernating animals

Lizards are ectotherms, like the other living reptiles. During hibernation, their metabolism, including growth and differentiation of the ovarian follicle, slows down (Filosa, '73). In hibernating animals, ovarian follicles show completely differentiated pyriform cells that exhibit a strong decrease of Ps-PL10 signal in the cytoplasm of oocytes (Fig. 9F) if compared to metabolically active animals (Fig. 8F and Fig. 9D).

DISCUSSION

We characterized and compared in the lizard *P. sicula* the expression pattern of two members of the DEAD-box family, one protein belonging to the DDX4/Vasa subfamily (Ps-VASA) (Milani and Maurizii, 2014, 2015) and one protein of the Ded1/DDX3 subfamily (Ps-PL10). This study represents the first report on PL10 expression pattern in reptilian germ cells of both sexes.

Analyses of the amino acid sequence supported that Ps-PL10 is a member of the Ded1/DDX3 subfamily, while Ps-VASA of the DDX4/Vasa subfamily (Figs. 1 and 2). Ps-VASA (Milani

and Maurizii, 2014, 2015) shows a different localization pattern compared to Ps-PL10 when analyzing the same reproductive phases (Table 2).

The main differences found are:

i) Ps-PL10 from spermatocytes/early oocytes, Ps-VASA from spermatogonia/oogonia;

ii) Ps-PL10 accumulation and disposal through residual bodies of late spermatids, Ps-VASA aggregation to the posterior portion of spermatid nucleus, close to mitochondrial midpiece;

iii) both the proteins appear absent in mature male gametes;

iv) both the proteins are present in follicular cells of the ovary that differentiate into pyriform cells (nurse-like cells).

For both the proteins, the staining appeared as granules/spots representing aggregation of molecules. Usually, very small stained granules can be seen before their aggregation in larger immunospots as soon as germ cell differentiation proceeds.

The observed differences support that the used anti-Ps-VASA and anti-Ps-PL10 actually react with different proteins. From the alignment (Fig. 1), it appears also evident that the sequences of immunogenic peptides are not shared between PL10 and p68 sequences, further supporting antibody specificity.

The detection of two close bands in Western blot using one or the other anti-PS-PL10 suggests the presence of two variants of the protein, slightly different in molecular weight. Further analyses should be performed to clarify this issue as soon as transcriptomes or the genome of *P. sicula* will be available.

Ps-PL10 is expressed in male meiotic cells and discarded with residual bodies

In adult testes, in agreement with mouse DDX3X protein localization (Sekiguchi et al., 2004), Ps-PL10 is present in several districts of the seminiferous tubules, as observed for PL10 in the mouse (Leroy et al., '89). A recent advance in this line of research shows how

murine PL10 is particularly involved in the pre-pachytene/pachytene phases of prophase I (Inoue et al., 2016). Accordingly, the expression of Ps-PL10 begins in spermatocytes located at the basal compartment of seminiferous epithelium; this expression time is particularly clear in the immature testis of *P. sicula*, when the wall of seminiferous tubules is forming. In this differentiation stage, few germ cells are present in the wall, allowing an easier localization of anti-Ps-PL10 signal in the cytoplasm of spermatocytes, while it is absent in spermatogonia (Fig. 7).

Anti-Ps-PL10 signal is low in germ cell early stages and increases during differentiation but becomes gradually confined into the removed residual bodies. Indeed, in adult testis, anti-Ps-PL10 staining is stronger at the apical region of the tubules where residual bodies are located. Some differences can be highlighted when compared to available data on vertebrates: in humans an Y-linked form of the protein is expressed at high levels in early spermatocytes, but shows its maximum in spermatogonia (Ditton et al., 2004; Gueler et al., 2012), differently from *P. sicula* in which they show no anti-Ps-PL10 signal. More similar the situation in the urochordate *Botryllus schlosseri*, in which the homologous protein BS-PL10 shows an expression climax during early spermatogenesis, and is absent in sperm (Rosner et al., 2006). Anyhow, all these reports suggest a role of Ded1/DDX3 proteins during spermatogenesis, as reported for other DEAD-box RNA helicases (e.g.: DDX4/Vasa, Tanaka et al. 2000; p68/DDX5, Lemaire and Heinlein, '93; gonadotropin-regulated testicular RNA helicase, GRTH/DDX25, Tsai-Morris et al., 2004), supporting for the protein family a general involvement in the process.

Noteworthy, during the spring, a strong Ps-PL10 staining accumulates in residual bodies (Figs. 4, 5, and 10; Supplementary Material 2). Spermatozoon differentiation envisages the segregation of most of the cytoplasmic mass into the residual body and its release during the last steps of differentiation; it does not have a nucleus and usually contains mitochondria,

ribosomes, membranes, vacuoles and vesicles (Breucker et al., '85). In *P. sicula*, in the period of full gonadic activity, unstained spermatozoa detach from Ps-PL10 immunostained residual bodies and are released in the tubule lumen (Fig. 4, Fig. 10). Consequently, during the regression of gonadic activity, the lumen is filled with residual bodies together with several stained cells (Fig. 5B,C; Supplementary Material 2). Accordingly, in Reptilia, the presence of cells sloughed off from epithelia and collected in the tubule lumen is well documented at the end of the reproductive season (Gribbins, 2011). The accumulation of spermatids in degeneration visible as apoptotic germ cells in clusters in the center of the lumen in mice (van der Weyden et al., 2006) has similarities with the cell clusters observed in *P. sicula*. This maintained clustering could be due to the persistence of intercellular bridges between germ cells up to the detachment of residual bodies, as described during human spermiogenesis (Breucker et al., '85).

In *P. sicula* male, Ps-VASA is expressed from spermatogonia to spermatids in which the protein aggregates at the posterior part of the nucleus (Milani and Maurizii, 2014, 2015), as documented for DDX4/Vasa (Sato et al., 2010) and GRTH/DDX25 in the mouse (Tsai-Morris et al., 2004; Sato et al., 2010). The aggregate was suggested to correspond to nuage material—namely the chromatoid body (CB) in spermatogenic cells—identified at the posterior part of developing spermatids also in mammals (Fawcett et al., '70; Shang et al., 2010). The fact that, in *P. sicula*, round spermatids do not show an evident anti-Ps-PL10 staining (Figs. 4B and 6), while it is abundant in the cytoplasm of late spermatids (Fig. 4D), may indicate that Ps-PL10 mainly act during the last phases of male gamete differentiation, after which it is promptly eliminated with residual bodies. Similarly, other proteins completed their activity during spermatogenesis and are then discarded from spermatids through residual bodies (see for example in mammals, Pan et al., 2005, and in *C. elegans*, Gleason et al., 2012).

Ps-PL10 expression from early meiotic cells to previtellogenic oocytes and in nourse cells

During *P. sicula* oogenesis, differently from Ps-VASA that is already present in oogonia, Ps-PL10 detection starts from the meiotic stages, whereas somatic cells of the GB stroma and somatic follicle cells result unstained. Ps-PL10 localization in pre-vitellogenic oocytes is comparable to what observed in *Xenopus*, where An3 (PL10) was detected in both cytoplasm and nucleus of pre-vitellogenic oocytes (Gururajan et al. ’94; Gururajan and Weeks, '97). However, in *Xenopus*, as well in the mouse, the protein localization was mostly detected in oocyte animal hemisphere (Sowden et al. '95). In *Drosophila*, Bel (PL10) colocalizes with VASA in the nuage at the posterior pole of the oocyte cytoplasm (Johnstone et al., 2005). In *P. sicula*, Ps-PL10 shows a subcortical-perinuclear localization but, in the stages analyzed, no germ plasm-like structure are detected by confocal microscope analysis, supporting the already proposed absence of localized nuage material in the oocytes of this species (Filosa and Taddei, '76 a,b).

The follicle cells that increase in size after their fusion with the oocyte, becoming firstly intermediate cells, then pyriform cells, express Ps-PL10 (Figs. 8 and 9; Supplementary Material 2). The presence of Ps-PL10, as well as Ps-VASA (Milani and Maurizii, 2015), in the nucleus and cytoplasm of these cells may be related to their function as nurse cells. In fact, pyriform cells are connected to the oocyte through intercellular bridges and are functionally related to *Drosophila* nurse cells (Taddei, '72). In *P. sicula*, the nurse cells differentiate from somatic follicle cells after their fusion with the oocyte (Andreuccetti et al., '78), differently from *Drosophila* in which they originate from the germ line (Koch and King, '66). As known, pyriform cells are functionally active in transferring RNAs together with cytoplasmic organelles into the oocyte (Taddei and Andreuccetti, '90; Motta et al., '95). Since

DEAD-box helicases are involved in RNA metabolism (Linder and Jankowsky, 2011; Linder and Fuller-Pace, 2013, 2015) and processes related to transport (Tseng et al., ’98; Hodge et al., ’99) – feature possibly extended to Ded1/DDX3 subfamily (Askjaer et al., '99, 2000; Yedavalli et al., 2004) – the expression of Ps-PL10 observed in the nuclei of pyriform cells of metabolically active animals may suggest a role of Ps-PL10 in the transport of RNA molecules from the nucleus to cytoplasm, as previously proposed for Ps-VASA (Milani and Maurizii, 2015). Similarly to Ps-VASA expression, the presence of Ps-PL10 in the cytoplasm of pyriform cells may indicate its involvement in the metabolism of RNA molecules that will be transferred through intercellular bridges into the oocyte; indeed, the cortical and subcortical regions of oocyte cytoplasm show Ps-PL10 stained granules (Fig. 9; Supplementary Material 2). In this connection, hibernating animals show a decreased Ps-PL10 signal, both in pyriform cells and in oocyte cytoplasm (Fig. 9F), if compared to metabolically active animals. The expression of Ps-PL10 in pyriform cells reminds what reported for *Drosophila*, where Bel (PL10) is localized both in nurse cells and in follicle cells (Johnstone et al., 2005), regardless of their germinal or somatic origin.

Interestingly, Ps-PL10 was detected also in the nucleoli of pyriform cells since the beginning of their differentiation (Figs. 8 and 9; Supplementary Material 2). The presence of Ded1/DDX3 in nucleoli may suggest a role in the processing of rRNA, as indicated by the finding of An3 in *Xenopus* oocytes in extranucleoli from late stages II through stage V, the stages in which transcription of rRNA is most active (Gururajan et al., 1994).

In conclusion, the obtained results indicate that Ps-PL10 may have a role in the differentiation process of *P. sicula* male and female germ cells. Differently to what reported in others animals, in which Ded1/DDX3 is detected also in Sertoli and interstitial cells (mouse; Sekiguchi et al., 2004), and follicular cells (*Drosophila*; Johnstone, 2005), Ps-PL10 is not expressed in somatic cells of the gonad in the analyzed stages; however, we cannot rule

out Ps-PL10 expression in other somatic tissues. As reported, DDX4/Vasa- and Ded1/DDX3 proteins show a wide range of expression patterns and studies focused on the identification and expression of orthologous genes will surely help in understanding the features observed in the different organisms and in the different developmental stages.

ACKNOWLEDGEMENTS

This study was supported by the Italian Ministry of Education, University and Research MIUR - SIR Programme no. RBSI14G0P5 funded to LM, and by RFO funding University of Bologna (2011/2012) funded to MGM. We would like to thank Monia Bentivogli for protein homogenate quantification, Augusto Giuseppe Lorenzo Foà, Cristiano Bertolucci, Elena Frigato who supplied specimens for Western blot analysis, and Katherina Orellana and Giorgio Modesti for the use of Leica TCS SP8 X. The authors have no conflict of interest to declare.

REFERENCES

Alié A, Leclère L, Jager M, et al. 2011. Somatic stem cells express *Piwi* and *Vasa* genes in an adult ctenophore: ancient association of "germline genes" with stemness. Dev Biol 350:183–97.

Andreuccetti P, Taddei C, Filosa S. 1978. Intercellular bridges between follicle cells and oocyte during the differentiation of follicular epithelium in *Lacerta sicula*. J Cell Sci 33:341–350.

Askjaer P, Bachi A, Wilm M, et al. 1999. RanGTP-regulated interactions of CRM1 with nucleoporins and a shuttling DEAD-box helicase. Mol Cell Biol 19:6276-6285.

Askjaer P, Rosendahl R, Kjems J. 2000. Nuclear export of the DEAD box An3 protein by CRM1 is coupled to An3 helicase activity. J Biol Chem 275:11561–11568.

Breucker H, Schäfer E, Holstein A-F. 1985. Morphogenesis and fate of the residual body in human spermiogenesis. Cell Tissue Res 240:303–309.

Chang T-C, Liu W-S. 2010. The molecular evolution of *PL10* homologs. BMC Evol Biol 10:127.

Chuang RY, Weaver PL, Liu Z, Chang TH. 1997. Requirement of the DEAD-Box protein Ded1p for messenger RNA translation. Science 275:1468–1471.

Ditton HJ, Zimmer J, Kamp C, Rajpert-De Meyts E, Vogt PH. 2004. The *AZFa* gene *DBY* (*DDX3Y*) is widely transcribed but the protein is limited to the male germ cells by translation control. Hum Mol Genet 13:2333-2341.

Fabioux C, Pouvreau S, Le Roux F, Huveta A. 2004. The oyster *vasa*-like gene: a specific marker of the germline in *Crassostrea gigas*. Biochem Bioph Res Co 315:897–904.

Fawcett DW, Eddy EM, Phillips DM. 1970. Observations on the fine structure and relationships of the chromatoid body in mammalian spermatogenesis. Biol Reprod 2:129–153.

Fierro-Constaín L, Schenkelaars Q, Gazave E, et al. 2017. The conservation of the germline multipotency program, from sponges to vertebrates: a stepping stone to understanding the somatic and germline origins. Genome Biol Evol. doi:10.1093/gbe/evw289.

Filosa S, Taddei C. 1976a. Intercellular bridges between germ-cells during the first stages of oogenesis in adult lizard. In: Progress in Differentiation Research (Muller-Berat, ed.). Amsterdam, pp. 261-263.

Filosa S, Taddei C. 1976b. Intercellular bridges in lizard oogenesis. Cell Diff 5:199–206.

Filosa S, Taddei C, Andreuccetti P. 1979. The differentiation and proliferation of follicle cells during oocyte growth in *Lacerta sicula*. J Embryol Exp Morphol 54:5–15.

Filosa S. 1973. Biological and cytological aspect of the ovarian cycle in *Lacerta sicula* Raf. Monitore Zool Ital 7:151–165.

Fischer S, Brunk BP, Chen F, et al. 2011. Using OrthoMCL to assign proteins to OrthoMCL-DB groups or to cluster proteomes into new ortholog groups. Curr Protoc Bioinformatics Chapter 6:Unit 6.12.1-19.

Ford MJ, Anton IA, Lane DP. 1988. Nuclear protein with sequence homology to translation initiation factor eIF-4A. Nature 332:736–738.

Foresta C, Ferlin A, Moro E. 2000. Deletion and expression analysis of *AZFa* genes on the human Y chromosome revealed a major role for *DBY* in male infertility. Hum Mol Genet 9:1161–1169.

Fujiwara Y, Komiya T, Kawabata H, et al. 1994. Isolation of a DEAD-family protein gene that encodes a murine homolog of *Drosophila* vasa and its specific expression in germ cell lineage. P Natl Acad Sci USA 91:12258–12262.

Fuller-Pace FV. 2006. DExD/H box RNA helicases: multifunctional proteins with important roles in transcriptional regulation. Nucleic Acids Res 34:4206–4215.

Gee SL, Conboy JG. 1994. Mouse erythroid cells express multiple putative RNA helicase genes exhibiting high sequence conservation from yeast to mammals. Gene 140:171–177.

Gleason EJ, Hartley PD, Henderson M, et al. 2012. Developmental genetics of secretory vesicle acidification during *Caenorhabditis elegans* spermatogenesis. Genetics 191: 477–491.

Gribbins KM. 2011. Reptilian spermatogenesis. A histological and ultrastructural perspective. Spermatogenesis 1:250–269.

Gueler B, Sonne SB, Zimmer J, et al. 2012. AZFa protein DDX3Y is differentially expressed in human male germ cells during development and in testicular tumours: new evidence for phenotypic plasticity of germ cells. Hum Reprod 27:1547–1555.

Gururajan R, Weeks DL. 1997. An3 protein encoded by a localized maternal mRNA in *Xenopus laevis* is an ATPase with substrate-specific RNA helicase activity. Biochim Biophys Acta 1350:169–182.

Gururajan R, Mathews L, Longo FJ, Weeks DL. 1994. An3 mRNA encodes an RNA helicase that colocalizes with nucleoli in *Xenopus* oocytes in a stage-specific manner. P Natl Acad Sci USA 91:2056–2060.

Gururajan R, Perry-O'Keefe HA, Melton DA, Weeks DL. 1991. The *Xenopus* localized messenger RNA An3 may encode an ATP-dependent RNA helicase. Nature 349:717–719.

Hirling H, Scheffner M, Restle T, Stahl H. 1989. RNA helicase activity associated with the human p68 protein. Nature 339:562–564.

Hodge CA, Colot H V, Stafford P, Cole CN. 1999. Rat8p/Dbp5p is a shuttling transport factor that interacts with Rat7p/Nup159p and Gle1p and suppresses the mRNA export defect of xpo1-1 cells. EMBO J 18:5778–5788.

Inoue H, Ogonuki N, Hirose M, et al. 2016. Mouse D1Pas1, a DEAD-box RNA helicase, is required for the completion of first meiotic prophase in male germ cells. Biochem Biophys Res Commun 478:592–598.

Johnstone O, Deuring R, Bock R, et al. 2005. Belle is a *Drosophila* DEAD-box protein required for viability and in the germ line. Dev Biol 277:92–101.

Jones RE, Swain T, Guillette LJ Jr, Fitzgerald KT. 1982. The comparative anatomy of lizard ovaries, with emphasis on the number of germinal beds. J Herpetol 16:240–252.

Koch EA, King RC. 1966. The origin and early differentiation of the egg chamber of *Drosophila melanogaster*. J Morphol. 119:283.

Komiya T, Itoh K, Ikenishi K, Furusawa M. 1994. Isolation and characterization of a novel gene of the DEAD box protein family which is specifically expressed in germ cells of *Xenopus laevis*. Dev Biol 162:354–363.

Kotov AA, Olenkina OM, Kibanov M V, Olenina L V. 2016. RNA helicase Belle (DDX3) is essential for male germline stem cell maintenance and division in *Drosophila*. Biochim Biophys Acta 1863:1093–1105.

Kozin VV, Kostyuchenko RP. 2015. *Vasa*, *PL10*, and *Piwi* gene expression during caudal regeneration of the polychaete annelid *Alitta virens*. Dev Genes Evol 225:129–138.

Kumar S, Stecher G, Tamura K. 2016. MEGA7: Molecular Evolutionary Genetics Analysis version 7.0 for bigger datasets. Mol Biol Evol 33:1870–1874.

Lasko PF, Ashburner M. 1988. The product of the *Drosophila* gene *vasa* is very similar to eukaryotic initiation factor-4a. Nature 335:611–617.

Leclère L, Jager M, Barreau C, et al. 2012. Maternally localized germ plasm mRNAs and germ cell/stem cell formation in the cnidarian *Clytia*. Developmental Biology 364:236–248.

Leininger S, Adamski M, Bergum B, et al. 2014. Developmental gene expression provides clues to relationships between sponge and eumetazoan body plans. Nat Commun 5:3905

Lemaire L, Heinlein U. 1993. High-level expression in male germ cells of murine P68 RNA helicase mRNA. Life Sci 52:917–926.

Leroy P, Alzari P, Sassoon D, Wolgemuth D, Fellous M. 1989. The protein encoded by a murine male germ cell-specific transcript is a putative ATP-dependent RNA helicase. Cell 57:549–559.

Linder P, Fuller-Pace F V. 2013. Looking back on the birth of DEAD-box RNA helicases. Biochim Biophys Acta 1829:750–755.

Linder P, Fuller-Pace F. 2015. Happy birthday: 25 years of DEAD-box proteins. Methods Mol Biol 1259:17–33.

Linder P, Jankowsky E. 2011. From unwinding to clamping - the DEAD box RNA helicase family. Nat Rev Mol Cell Biol12:505–516.

Linder P, Lasko PF, Ashburner M, et al. 1989. Birth of the D-E-A-D box. Nature 337:121–122.

Linder P, Tanner NK, Banroques J. 2001. From RNA helicases to RNPases. Trends Biochem Sci 26:339–341.

Linder P. 2006. Dead-box proteins: a family affair—active and passive players in RNP-remodeling. Nucleic Acids Res 34:4168–4180.

Lowry OH, Rosebrough NJ, Farr AL, Randall R. 1951. Protein measurement with the Folin phenol reagent. J Biol Chem 193:265–275.

Marracci S, Casola C, Bucci S, et al. 2007. Differential expression of two *vasa/PL10*-related genes during gametogenesis in the special model system *Rana*. Dev Genes Evol 217:395–402.

Maurizii MG, Cavaliere V, Gamberi C, et al. 2009. Vasa protein is localized in the germ cells and in the oocyte-associated pyriform follicle cells during early oogenesis in the lizard *Podarcis sicula*. Dev Genes Evol 219:361–367.

Milani L, Maurizii MG. 2014. First evidence of Vasa expression in differentiating male germ cells of a reptile. Mol Reprod Dev 81:390.

Milani L, Maurizii MG. 2015. Vasa expression in spermatogenic cells during the reproductive-cycle phases of *Podarcis sicula* (Reptilia, Lacertidae). J Exp Zool Part B 324:424–434.

Mitchell A, Chang H-Y, Daugherty L, et al. 2015. The InterPro protein families database: the classification resource after 15 years. Nucleic Acids Res 43:D213–D221.

Mochizuki K, Nishimiya-Fujisawa C, Fujisawa T. 2001. Universal occurrence of vasa-related genes among metazones and their germline expression in *Hydra*. Dev Genes Evol 211:299–308.

Motta CM, Castriota Scerberg M, Filosa S, Andreuccetti P. 1995. Role of pyriform cells during the growth of oocytes in the lizard *Podarcis sicula*. J Exp Zool 273:247–256

Olsen LC, Aasland R, Fjose A. 1997. A *vasa*-like gene in zebrafish identifies putative primordial germ cells. Mech Dev 66:95–105.

Pan J, Goodheart M, Chuma S, et al. 2005. RNF17, a component of the mammalian germ cell nuage, is essential for spermiogenesis. Development 132:4029–4039.

Park SH, Lee S-G, Kim Y, Song K. 1998. Assignment of a human putative RNA helicase gene, DDX3, to human X chromosome bands p11.3→p11.23. Cytogenet Genome Res 81:178–179.

Raz E. 2000. The function and regulation of *vasa*-like genes in germ cell development. Genome Biol 1:1017.1–1017.6

Rauschendorf M-A, Zimmer J, Ohnmacht C, Vogt PH. 2014. *DDX3X*, the X homologue of AZFa gene *DDX3Y*, expresses a complex pattern of transcript variants only in the male germ line. Mol Hum Reprod 20:1208–1222.

Rocak S, Linder P. 2004. DEAD-box proteins: the driving forces behind RNA metabolism. Nat Rev Mol Cell Biol 5:232–241.

Rebscher N, Zelada-González F, Banisch TU, Raible F, Arendt D. 2007.Vasa unveils a common origin of germ cells and of somatic stem cells from the posterior growth zone in the polychaete *Platynereis dumerilii*. Dev Biol 306:599–611.

Rosner A, Paz G, Rinkevich B. 2006. Divergent roles of the DEAD-box protein BS-PL10, the urochordate homologue of human DDX3 and DDX3Y proteins, in colony astogeny and ontogeny. Dev Dyn 235:1508–1521.

Rosner A, Rinkevich B. 2007. The DDX3 subfamily of the DEAD box helicases: Divergent roles as unveiled by studying different organisms and in vitro assays. Curr Med Chem 14:2517–25.

Sato H, Tsai-Morris C-H, Dufau ML. 2010. Relevance of gonadotropin-regulated testicular RNA helicase (GRTH/DDX25) in the structural integrity of the chromatoid body during spermatogenesis. Biochim Biophys Acta 1803:534–543.

Schindelin J, Arganda-Carreras I, Frise E, Kaynig V, et al. 2012. Fiji: an open-source platform for biological-image analysis. Nat Methods 9:676–682.

Schmid SR, Linder P. 1992. D-E-A-D protein family of putative RNA helicases. Mol Microbiol 6:283–291.

Shang P, Baarends WM, Hoogerbrugge J, et al. 2010. Functional transformation of the chromatoid body in mouse spermatids requires testis-specific serine/threonine kinases. J Cell Sci 123:331–339.

Sekiguchi T, Iida H, Fukumura J, Nishimoto T. 2004. Human DDX3Y, the Y-encoded isoform of RNA helicase DDX3, rescues a hamster temperature-sensitive ET24 mutant cell line with a DDX3X mutation. Exp Cell Res 300:213–222.

Sharma D, Jankowsky E. 2014. The Ded1/DDX3 subfamily of DEAD-box RNA helicases. Crit Rev Biochem Mol Biol 49:343–360.

Siebert S, Goetz FE, Church SH, et al. 2015. Stem cells in *Nanomia bijuga* (Siphonophora), a colonial animal with localized growth zones. EvoDevo 6:22.

Sowden J, Putt W, Morrison K, Beddington R, Edwards Y. 1995. The embryonic RNA helicase gene (ERH): a new member of the DEAD box family of RNA helicases. Biochem J 308:839–846.

Skinner DE, Rinaldi G, Suttiprapa S, et al. 2012. Vasa-Like DEAD-Box RNA Helicases of *Schistosoma mansoni*. PLoS Negl Trop Dis 6:e1686.

Solana J, Romero R. 2009. SpolvlgA is a DDX3/PL10-related DEAD-box RNA helicase expressed in blastomeres and embryonic cells in planarian embryonic development. Int J Biol Sci 5:64–73.

Taddei C, Andreuccetti P. 1990. Structural modifications of the nuclear components during lizard oogenesis in relation to the differentiation of the follicular epithelium. Cell Differ Dev 29:205–215.

Taddei C. 1972. Significance of pyriform cells in the ovarian follicle of *Lacerta sicula*. Exp Cell Res 72:562–566.

Tanaka SS. et al. 2000. The mouse homolog of *Drosophila Vasa* is required for the development of male germ cells. Gene Dev 14:841–853.

Tsai-Morris C-H, Sheng Y, Lee E, Lei K-J, Dufau ML. 2004. Gonadotropin-regulated testicular RNA helicase (GRTH/Ddx25) is essential for spermatid development and completion of spermatogenesis. P Natl Acad Sci USA 101:6373–6378.

Tseng SS, Weaver PL, Liu Y, et al. 1998. Dbp5p, a cytosolic RNA helicase, is required for poly(A)+ RNA export. EMBO J 17:2651–2662.

Tsunekawa N, Naito M, Sakai Y, Nishida T, Noce T. 2000. Isolation of chicken *vasa* homolog gene and tracing the origin of primordial germ cells. Development 127:2741–2750.

van der Weyden L, Arends MJ, Chausiaux OE, et al. 2006. Loss of TSLC1 Causes Male Infertility Due to a Defect at the Spermatid Stage of Spermatogenesis. Mol Cell Biol 26:3595–3609.

Vong QP, Li Y, Lau Y-FC, et al. 2006. Structural characterization and expression studies of *Dby* and its homologs in the mouse. J Androl 27:653–661.

Wang Q, Fang D-A, Sun J-L, et al. 2012. Characterization of the *vasa* gene in the Chinese mitten crab *Eriocheir sinensis*: A germ line molecular marker. J Insect Physiol 58:960–965.

Yajima M, Wessel GM. 2015. Essential elements for translation: the germline factor Vasa functions broadly in somatic cells. Development 142:1960–1970.

Yedavalli VSRK, Neuveut C, Chi Y-H, Kleiman L, Jeang K-T. 2004. Requirement of DDX3 DEAD box RNA helicase for HIV-1 Rev-RRE export function. Cell 119:381–392.

Zhou Q, Shao M, Qin Z, Kang KH, Zhang Z. 2010. Cloning, characterization, and expression analysis of the DEAD-box family genes, *Fc-vasa* and *Fc-PL10a*, in Chinese shrimp (*Fenneropenaeus chinensis*)*. Chin J Oceanol Limn 28:37–45.

).

FIGURE LEGENDS

Figure 1. PL10 protein alignment. Amino acid partial sequence of *Podarcis sicula* PL10 (Ps-PL10) aligned with some orthologs. Identity in black, similarities in gray/white. Ps-PL10 peptides used for antibody production are highlighted (YEE and DAL starting sequences), as well as DEAD-box protein domains (according to InterPro analysis).

Figure 2. Phylogenetic tree of closely related subfamilies of DEAD-box proteins. Four-five amino acid sequences belonging to p68/DDX5, Ded1/DDX3, DDX4/Vasa subfamilies, depending on the availability, from the major living gnathostomes, were selected, trying to maintain the same representative species among the subfamilies. Maximum Likelihood (bootstrap values on the top of main nodes) and Neighbour Joining (bootstrap values on the bottom of main nodes) trees, calculated with Mega 7 (1,000 bootstrap replicates), showed a comparable topology. (Sequence alignment in Supplementary Material 1).

Figure 3. Anti-Ps-PL10 antibody specificity: Western blots of ovary and testis extracts of *P. sicula*. (A) From the right to the left: protein standard (St), Western blot of testis extract, Western blot of ovary extract. Anti-Ps-PL10-YEE detected two bands (72 and 70 kDa) in ovary extract and one band (72 kDa) in testis extract. (B) Western blots of ovary and testis extracts using anti-Ps-PL10-YEE and anti-Ps-PL10-DAL. Both the antibodies detected one or two protein bands of about 70 and 72 kDa. These bands result strongly reduced when the antibodies are incubated with the immunogenic peptides. (See also Supplementary Material 2).

Figure 4. Ps-PL10 protein localization in male germ cells during full gonadic activity (in the spring). (A) cross section of a seminiferous tubules in which the wall of the epithelium shows different generations of germ cells: spermatogonia (sg), close to the basal membrane and, in succession, a large population of spermatocytes I (scI) and II (scII), and many stages of spermatids (st) in differentiation, evident in the apical region of the tubule. In the lumen (lu) mature spermatozoa (s) are present. (B) At higher magnification (dashed square in A), mature spermatozoa (s) in the tubule lumen result completely unstained. (C) Ps-PL10 immunostaining is present in spermatocytes (scI and scII), while spermatogonia (sg) and somatic cells (Sertoli cells, Se) result unstained. (D) At higher magnification (dotted square in A scanned at a different depth), late spermatids (lst) at the final stages of differentiation, localized at the apical region near the tubule lumen, show a strong Ps-PL10 staining in their cytoplasm: residual body (rb), spermatid nucleus (n) (see also Fig. 10). Anti-Ps-PL10 in red, TO-PRO 3 nuclear dye in green.

Figure 5. Ps-PL10 localization in male germ cells during regression of gonadic activity (in the summer). (A) A seminiferous tubule transversely sectioned showing in the apical region and in the tubule lumen many residual bodies strongly immunostained (arrowhead). Only few spermatozoa (s) are present in the lumen and resulted unstained (magnified in the inset on the right). In the basal compartment, only spermatocytes (sc) result immunolabeled, while spermatogonia (sg) are unstained (dashed square, magnified in the inset on the left); some spermatogonia are in proliferative activity (dashed oval). (B) A tubule lumen in which many Ps-PL10-immunostained residual bodies (arrow) and a cluster of spermatids probably in degeneration (asterisk) are present. In the intratubular spaces some erythrocytes (e) with endogenous fluorescence are visible. (C) Magnification of the tubule lumen in B. (See also Supplementary Material 2). Anti-Ps-PL10 in red, TO-PRO 3 nuclear dye in green.

Figure 6. Ps-PL10 localization in male germ cells during slow autumnal recrudescence. (A) The wall of the seminiferous epithelium increases in thickness and each stage of germ cell differentiation is present, with an abundance of spermatogonia (sg) and spermatocytes (sc) (spermatids: st). The lumen is small with few unstained spermatozoa (s). (B) Magnification of the tubule wall showing Ps-PL10 expression only in spermatocytes (sc). Anti-Ps-PL10 in red, TO-PRO 3 nuclear dye in green.

Figure 7. Ps-PL10 localization in male germ cells in immature testes (in November). (A) Cross section of an immature testis showing many seminiferous tubules (one is circled) during the wall organization. (B) Ps-PL10 expression is present in spermatocytes (sc), while the more peripheral spermatogonia (sg) resulted unstained. Anti-Ps-PL10 in red, TO-PRO 3 nuclear dye in green.

Figure 8. Ps-PL10 localization in female germ cells in the germinal bed (A-E) and in the previtellogenic ovarian follicle (F). (A) Sagittal section of the germinal bed (GB) of an ovary showing germ cells, at different stages of differentiation, dispersed in the somatic cells of the stroma (sc). In the dashed square, a cluster of germ cells with roundish nucleus, like oogonia (arrowhead); in the dotted square, other cells with dispersed chromatin, likely early meiotic cells. Some isolated early diplotenic oocytes (one in the dashed circle) are present. Just underneath the GB, an early follicle, characterized by a monolayered follicular cells (fc), around a developing oocyte (Oo), is evident. (B) A magnification of a GB region showing granules of Ps-PL10 dispersed in the cytoplasm of early oocytes (dashed circle), while the somatic cells (sc) of the stroma result unstained. (C) Merge of a single optical section (magnification from A), showing an early follicle of about 100 μm in diameter. Numerous

Ps-PL10-immunostained spots are present in the oocyte cytoplasm (Oo), while the surrounding somatic follicular cells (fc) result unstained; some enlarged follicular cells (intermediate cells) show a weak Ps-PL10 signal in their cytoplasm (dashed rectangle and inset). (D) Red channel projection that shows a weak Ps-PL10 signal in the nucleolus of an intermediate cell (dashed oval) when visualized through the “royal” Fiji Lookup Table (LUT) (see also Supplementary Material 2). The strong signal in (*) corresponds to an autofluorescent erithrocyte. (E) Z-projection of the same follicle in C, where Ps-PL10 spots of bigger dimensions are concentrated in a well evident perinuclear region in the oocyte (Oo). The nuclear region is circled; follicular cells (fc) are unstained. (F) 3D-projection of a portion of a bigger follicle showing the perinuclear localization of many stained spots (dashed oval) in the oocyte cytoplasm (Oo). The arrowhead points to the position of the oocyte nucleus; follicular cells (fc) are unstained. Anti-Ps-PL10 in red, TO-PRO 3 nuclear dye in green.

Figure 9. Ps-PL10 localization in germ cells of ovarian follicles of metabolically active animals (A-E) and hibernating animals (F). (A) Ovarian follicle of about 300 μm in diameter in which some follicle cells, in contact with the oocyte surface, enlarge (intermediate cells; dashed square) after their fusion with the oocyte (Oo). (B) Higher magnification of an intermediate cell (ic) of an ovarian follicle, corresponding to that boxed in A, in which few Ps-PL10-immunostained spots are present in the cytoplasm. (C) Ovarian follicle of about 800-1,000 μm in diameter. In the multilayered follicular epithelium, intermediate cells (ic) and pyriform cells (pc) are connected, through intercellular bridges (asterisks), to the oocyte (Oo). Small follicle cells (arrowhead) are localized in different districts of the epithelium. (D) Ovarian follicle, corresponding to that shown in C, in which numerous spots of Ps-PL10 are present in the cytoplasm of intermediate (ic), pyriform cells (pc), and in the oocyte cortical region (Oo). Some spots are also present in the nuclei of intermediate and pyriform cells

(asterisks). Small follicle cells (arrowhead) result unstained. (E) Merge of a single optical section of the follicular epithelium corresponding to that shown in (D), in which, at high magnification, the Ps-PL10 signal is detected in the nucleus of pyriform cells (magnified in the inset) (see also Supplementary Material 2). (F) Ovarian follicle of hibernating animals of about 800 μm in diameter showing a strong reduction of Ps-PL10 expression in the cytoplasm of intermediate (ic), pyriform cells (pc), and in oocyte cytoplasm (Oo). (A, C) Microtubules (anti-α-tubulin) in green, TO-PRO 3 nuclear dye in red. (B, D, E, F) Anti-Ps-PL10 in red, TO-PRO 3 nuclear dye in green.

Figure 10. Scheme of spermiogenesis. During spermiogenesis, (A) the spermatid undergoes a series of morphological modifications including: (B) the nucleation of the flagellum, (C) the acrosome formation, and (D) a deep reorganization in which the majority of the cell content, including organelles, are discarded through the residual body, that is essentially a large cytoplasmic vesicle.

Supplementary Material 1. Alignment used for the phylogenetic analysis.

Supplementary Material 2. Ps-PL10 localization using anti-Ps-PL10-DAL in *Podarcis sicula* testis and ovary (summer, late July), and controls.

Table 1. Examples of animals in which data on Ded1/DDX3 family are available

Species	Ded1/DDX3 gene name	Reference
Sycon ciliatum (Porifera)	*pl10*	Leininger et al., 2014
Pleurobrachia pileus (Ctenophora)	*PpiPL10*	Alié et al., 2011
Hydra magnipapillata (Cnidaria)	*CnPL10*	Mochizuki et al., 2001
Clytia (Cnidaria)	*PL10*	Leclère et al., 2012
Nanomia bijuga (Cnidaria)	*pl10*	Siebert et al., 2015
Schmidtea polychroa (Platyhelminthes)	*SpolvlgA*	Solana and Romero, 2009
Schistosoma mansoni (Platyhelminthes)	*Smvlg1, Smvlg2, Smvlg3*	Skinner et al., 2012
Platynereis dumerilii (Annelida)	Pdu-PL10	Rebscher et al., 2007
Alitta virens (Annelida)	*PL10*	Kozin and Kostyuchenko, 2015
Drosophila (Arthropoda)	Bel	Johnstone et al., 2005
Botryllus schlosseri (Chordata)	BS-PL10	Rosner et al., 2006
Zebrafish (Chordata)	*pl10a*	Olsen et al., '97
Xenopus (Chordata)	*an3*	Gururajan et al., '91
Rana esculenta complex (Chordata)	*RlPL10*	Marracci et al., 2007
Mouse (Chordata)	D1Pas1 (Pl10)	Vong et al., 2006
	DBY (DDX3Y)	Sowden et al., '95
	DDX3 (DDX3X)	Sowden et al., '95
Human (Chordata)	DBY (DDX3Y)	Foresta et al., 2000
	DDX3 (DDX3X)	Park et al. '98
		Rauschendorf et al., 2014

Table 2. Pattern of localization of Ps-PL10 and Ps-VASA in *Podarcis sicula* male and female gonads

Cell type	Proteins		Subcellular localization	
	PL10	**VASA**	**PL10**	**VASA**
Male				
spermatogonia	-	+	-	cytoplasmic spots
spermatocytes	+	++	cytoplasmic spots	cytoplasmic spots
late spermatids	++	++	cytoplasm to the residual body	between spermhead and flagellum
residual bodies	+++	-	Strongly diffused in the cytoplasm	-
spermatozoa	-	-	-	-
somatic cells	-	-	-	-
Female				
oogonia	-	+++	cytoplasmic spots	cytoplasm
early meiotic oocytes	+	+++	cytoplasmic spots	cytoplasm
developing/big oocytes	+	++	cytoplasmic spots	cytoplasmic spots
somatic cells of the stroma	-	-	-	-
somatic cells of the follicle	-	-	-	-
intermediate cells	+	++	cytoplasmic, nuclear, and nucleolar spots	cytoplasmic and nuclear spots
pyriform cells	+	++	cytoplasmic, nuclear, and nucleolar spots	cytoplasmic and nuclear spots

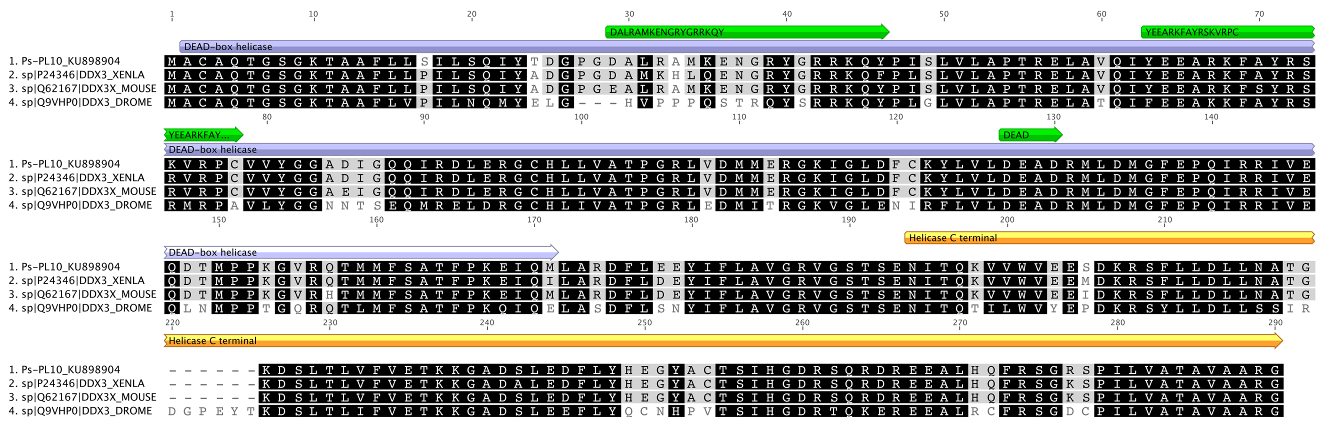

DEAD-box helicase
DALRAMKENGRYGRRKQY
YEEARKFAYRSKVRPC
YEEARKFAY...
DEAD
Helicase C terminal
1. Ps-PL10_KU898904
2. sp|P24346|DDX3_XENLA
3. sp|Q62167|DDX3X_MOUSE
4. sp|Q9VHP0|DDX3_DROME

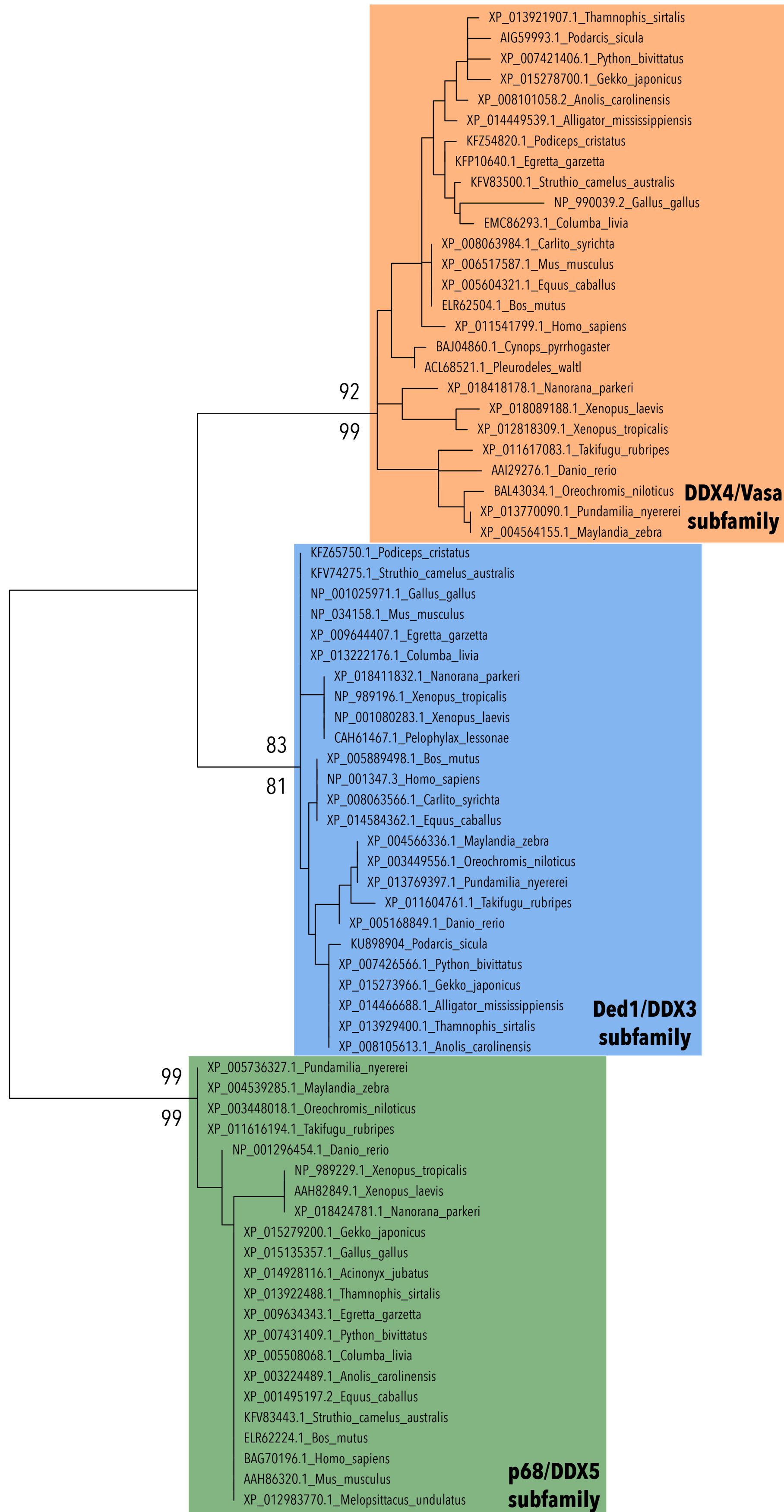
XP_013921907.1_Thamnophis_sirtalis
AIG59993.1_Podarcis_sicula
XP_007421406.1_Python_bivittatus
XP_015278700.1_Gekko_japonicus
XP_008101058.2_Anolis_carolinensis
XP_014449539.1_Alligator_mississippiensis
KFZ54820.1_Podiceps_cristatus
KFP10640.1_Egretta_garzetta
KFV83500.1_Struthio_camelus_australis
NP_990039.2_Gallus_gallus
EMC86293.1_Columba_livia
XP_008063984.1_Carlito_syrichta
XP_006517587.1_Mus_musculus
XP_005604321.1_Equus_caballus
ELR62504.1_Bos_mutus
XP_011541799.1_Homo_sapiens
BAJ04860.1_Cynops_pyrrhogaster
ACL68521.1_Pleurodeles_waltl
92
99
XP_018418178.1_Nanorana_parkeri
XP_018089188.1_Xenopus_laevis
XP_012818309.1_Xenopus_tropicalis
XP_011617083.1_Takifugu_rubripes
AAI29276.1_Danio_rerio
BAL43034.1_Oreochromis_niloticus
XP_013770090.1_Pundamilia_nyererei
XP_004564155.1_Maylandia_zebra
DDX4/Vasa subfamily
KFZ65750.1_Podiceps_cristatus
KFV74275.1_Struthio_camelus_australis
NP_001025971.1_Gallus_gallus
NP_034158.1_Mus_musculus
XP_009644407.1_Egretta_garzetta
XP_013222176.1_Columba_livia
XP_018411832.1_Nanorana_parkeri
NP_989196.1_Xenopus_tropicalis
NP_001080283.1_Xenopus_laevis
CAH61467.1_Pelophylax_lessonae
83
81
XP_005889498.1_Bos_mutus
NP_001347.3_Homo_sapiens
XP_008063566.1_Carlito_syrichta
XP_014584362.1_Equus_caballus
XP_004566336.1_Maylandia_zebra
XP_003449556.1_Oreochromis_niloticus
XP_013769397.1_Pundamilia_nyererei
XP_011604761.1_Takifugu_rubripes
XP_005168849.1_Danio_rerio
KU898904_Podarcis_sicula
XP_007426566.1_Python_bivittatus
XP_015273966.1_Gekko_japonicus
XP_014466688.1_Alligator_mississippiensis
XP_013929400.1_Thamnophis_sirtalis
XP_008105613.1_Anolis_carolinensis
Ded1/DDX3 subfamily
99
99
XP_005736327.1_Pundamilia_nyererei
XP_004539285.1_Maylandia_zebra
XP_003448018.1_Oreochromis_niloticus
XP_011616194.1_Takifugu_rubripes
NP_001296454.1_Danio_rerio
NP_989229.1_Xenopus_tropicalis
AAH82849.1_Xenopus_laevis
XP_018424781.1_Nanorana_parkeri
XP_015279200.1_Gekko_japonicus
XP_015135357.1_Gallus_gallus
XP_014928116.1_Acinonyx_jubatus
XP_013922488.1_Thamnophis_sirtalis
XP_009634343.1_Egretta_garzetta
XP_007431409.1_Python_bivittatus
XP_005508068.1_Columba_livia
XP_003224489.1_Anolis_carolinensis
XP_001495197.2_Equus_caballus
KFV83443.1_Struthio_camelus_australis
ELR62224.1_Bos_mutus
BAG70196.1_Homo_sapiens
AAH86320.1_Mus_musculus
XP_012983770.1_Melopsittacus_undulatus
p68/DDX5 subfamily
0.09

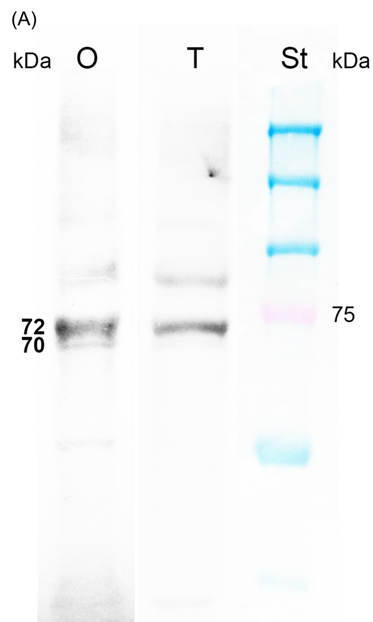
(A)
kDa
O
T
St
kDa
72
70
75

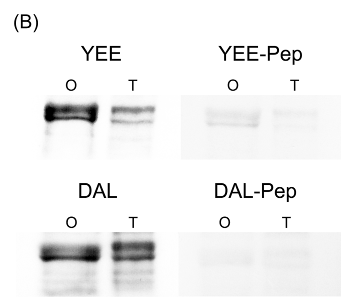
(B)
YEE
O
T
YEE-Pep
O
T
DAL
O
T
DAL-Pep
O
T

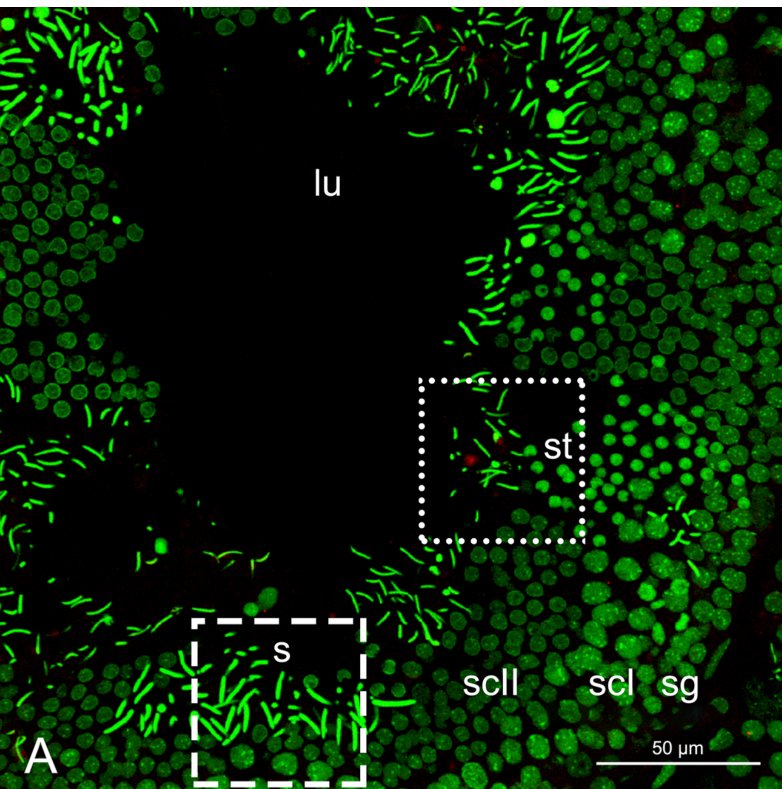
lu
st
s
scII
scI
sg
50 µm
A
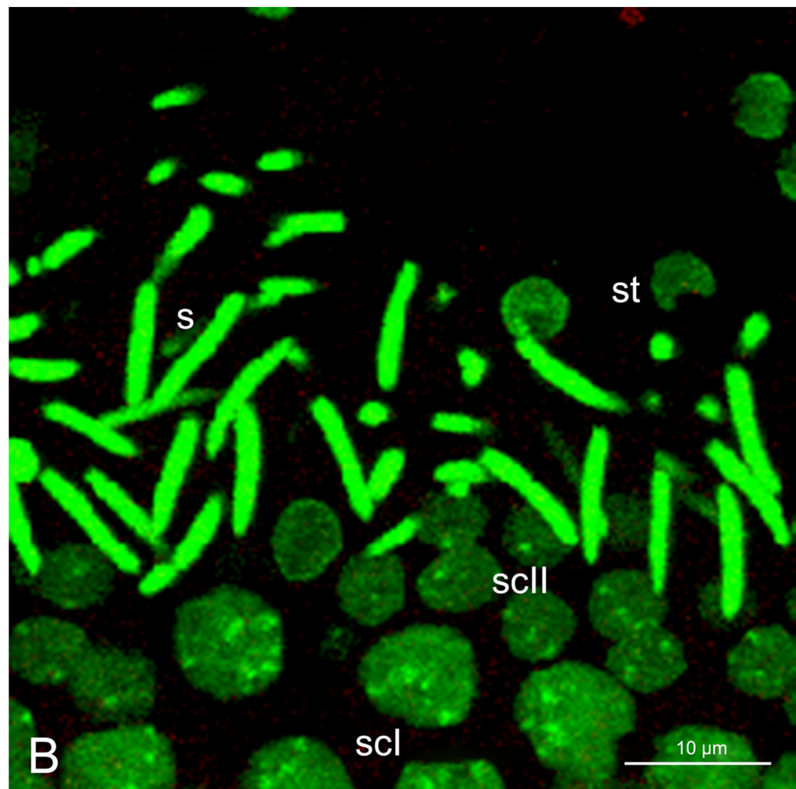
st
s
scII
scI
10 µm
B
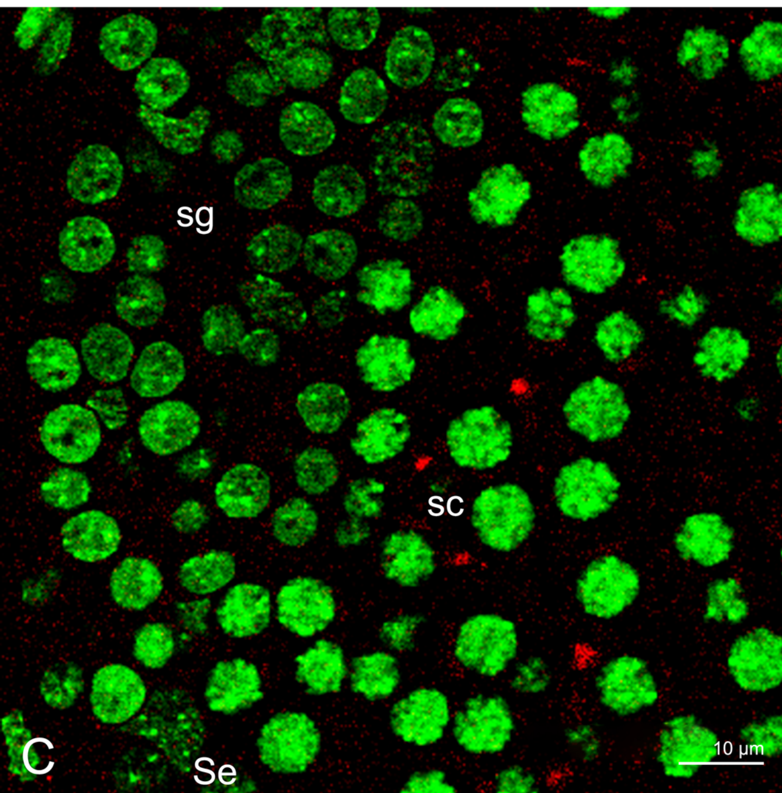
sg
sc
Se
10 µm
C
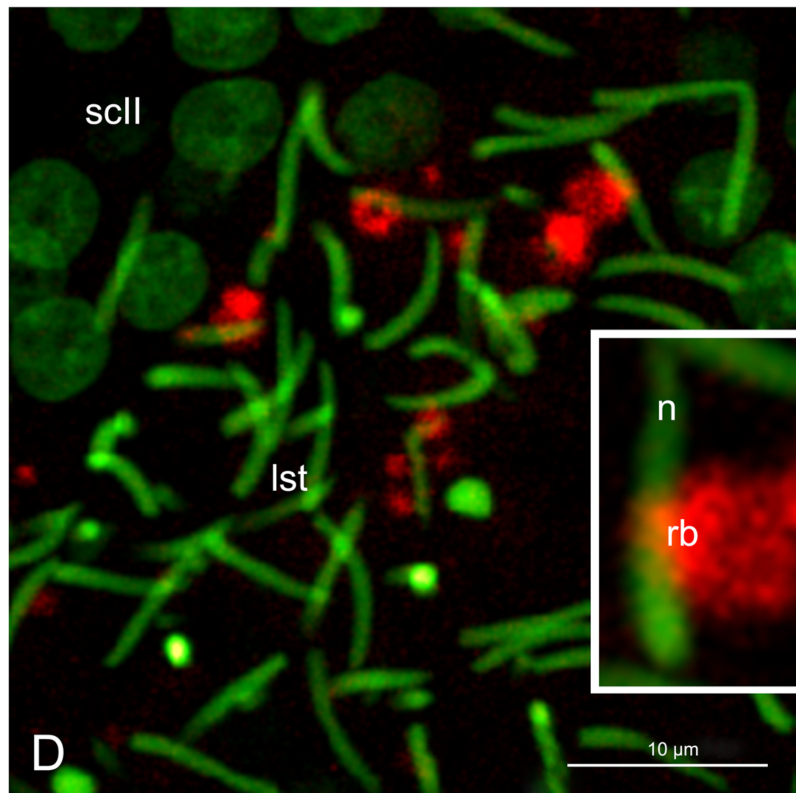
scII
lst
n
rb
10 µm
D

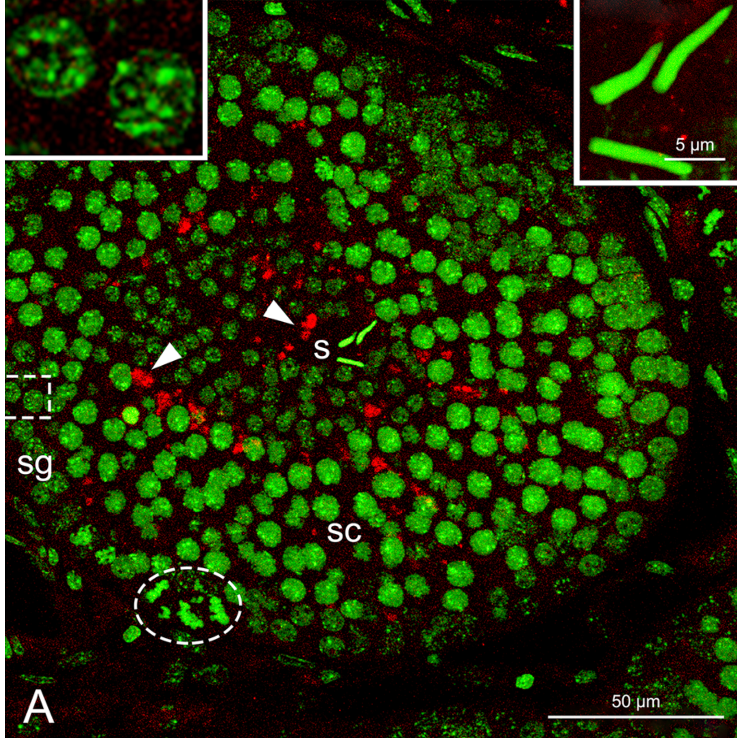

5 µm
s
sg
sc
A
50 µm

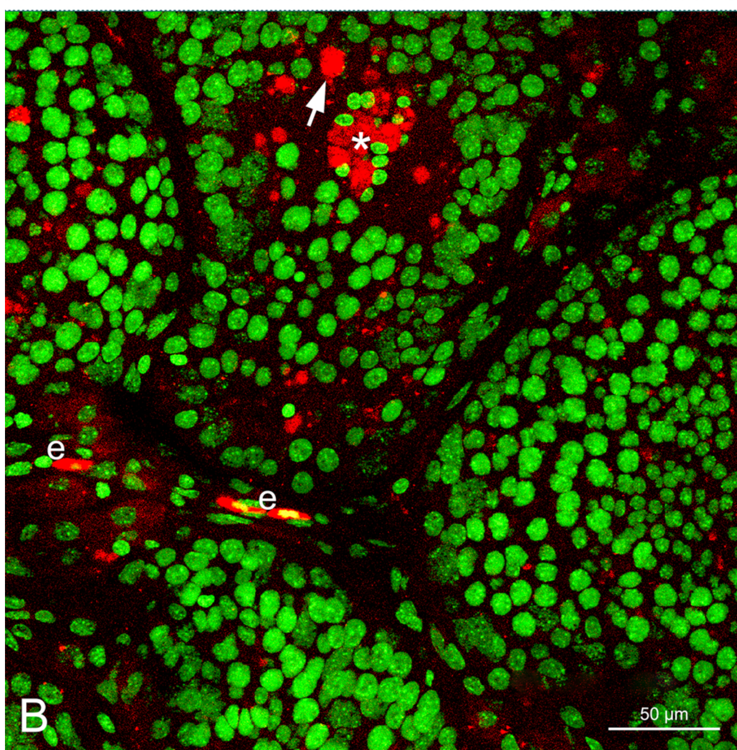

*
e
e
B
50 µm

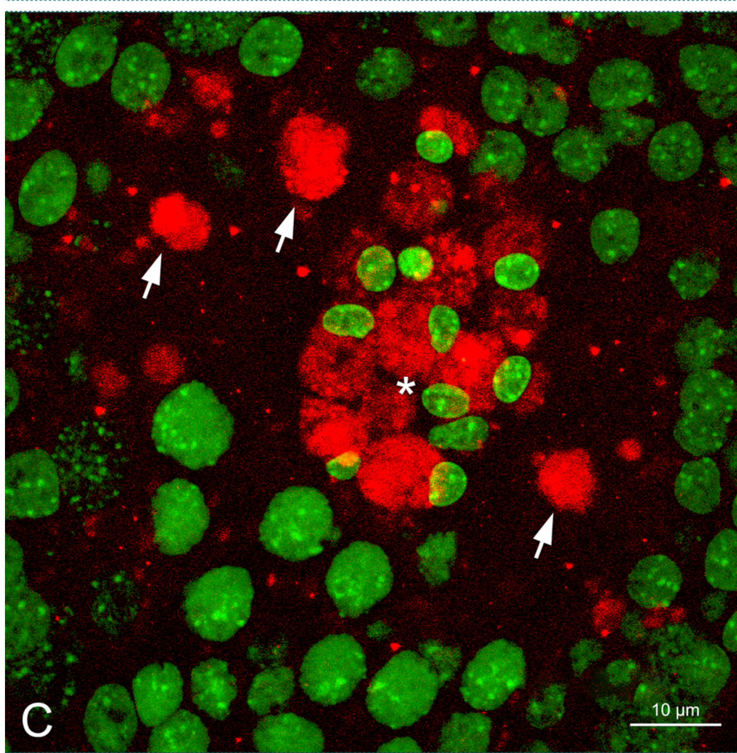

*
C
10 µm

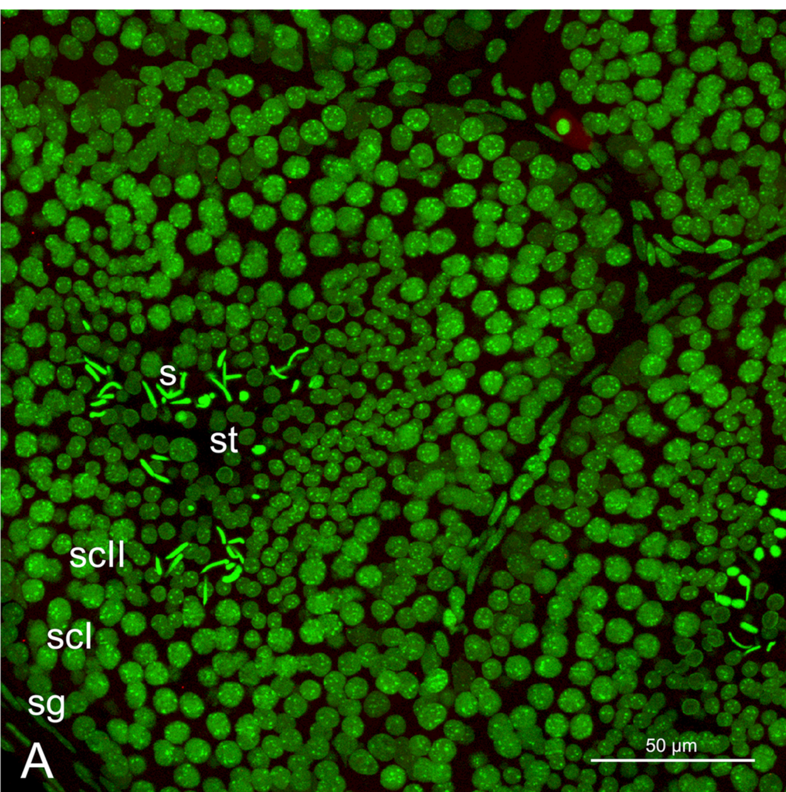
s
st
scII
scI
sg
A
50 µm

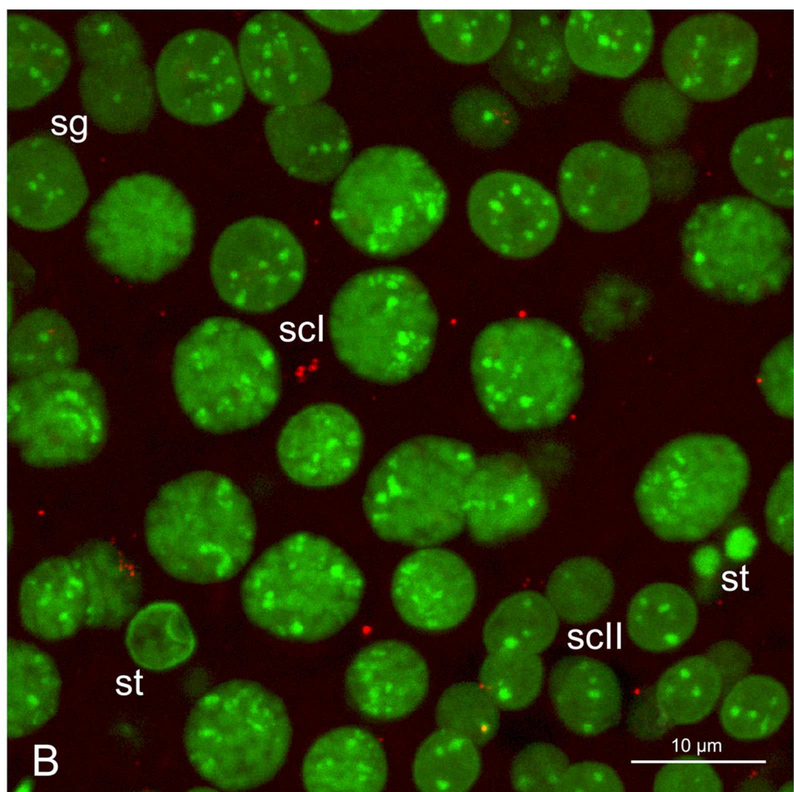
sg
scI
st
st
scII
B
10 µm

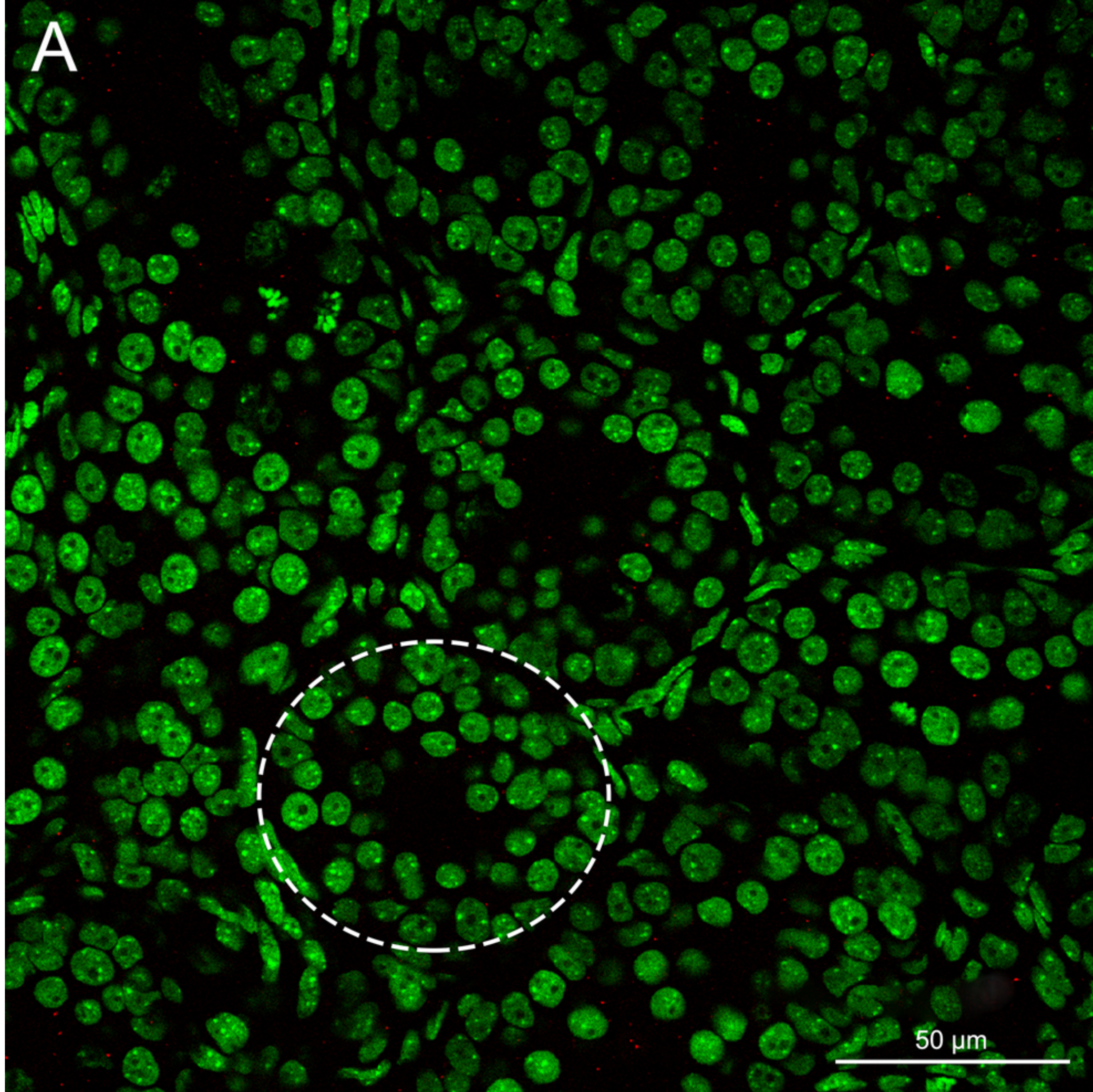
A
50 µm

B
sc
sg
10 µm

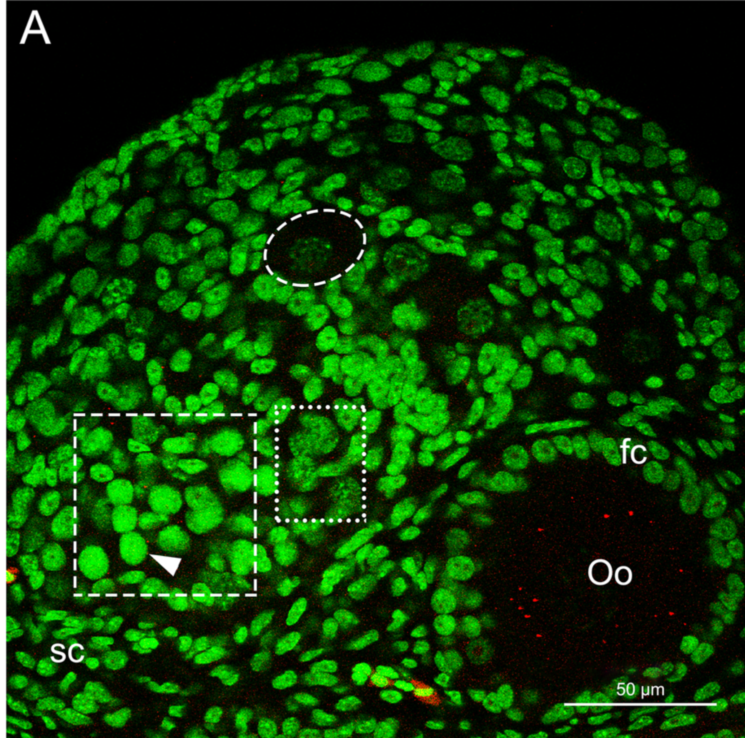
A
fc
Oo
sc
50 µm

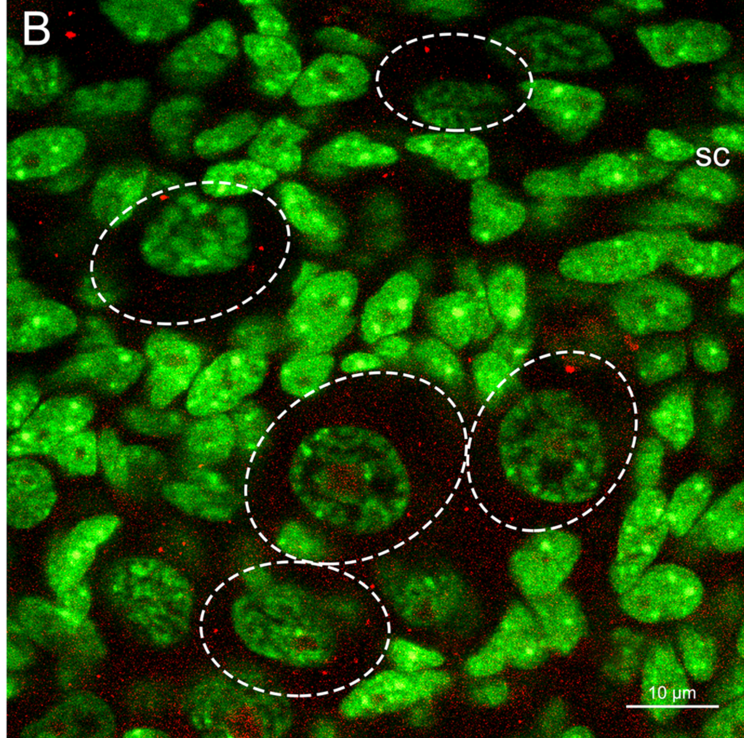
B
sc
10 µm

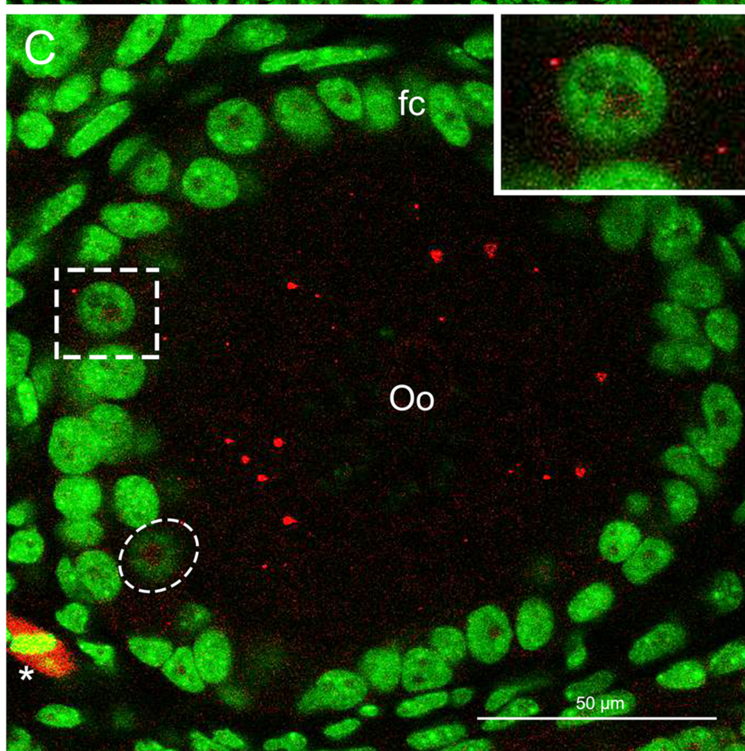
C
fc
Oo
*
50 µm

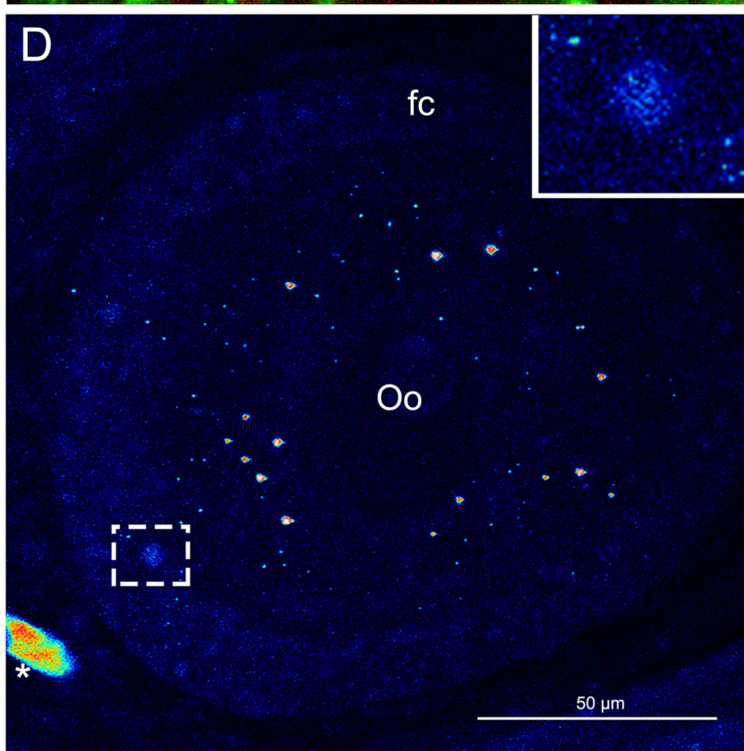
D
fc
Oo
*
50 µm

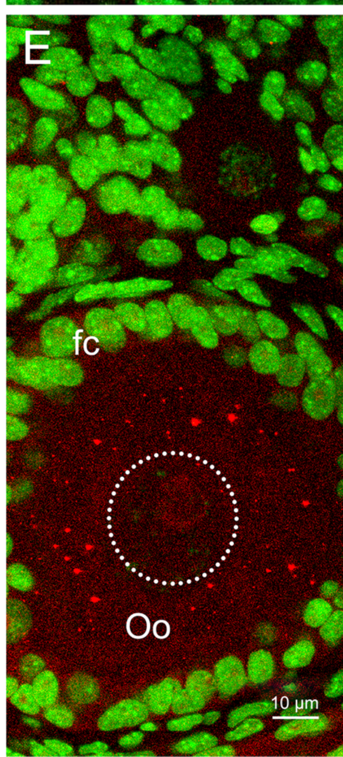
E
fc
Oo
10 µm

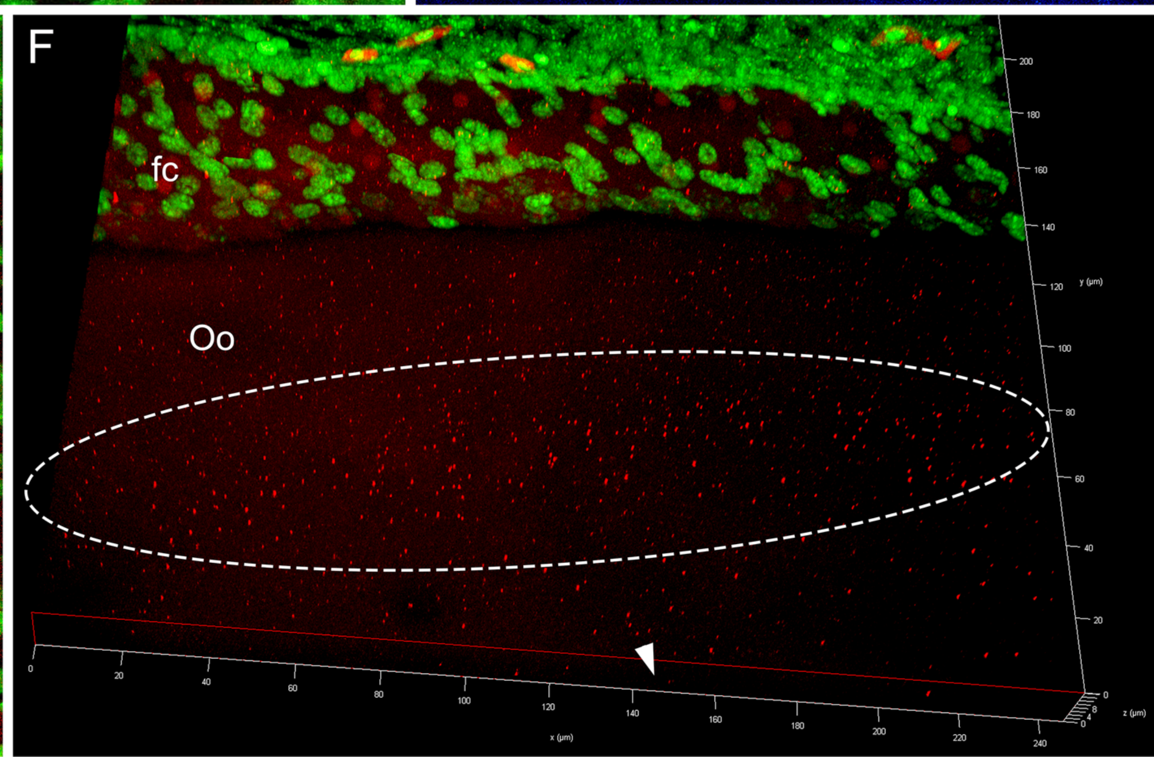
F
fc
Oo
y (µm)
x (µm)
z (µm)
0
20
40
60
80
100
120
140
160
180
200
220
240

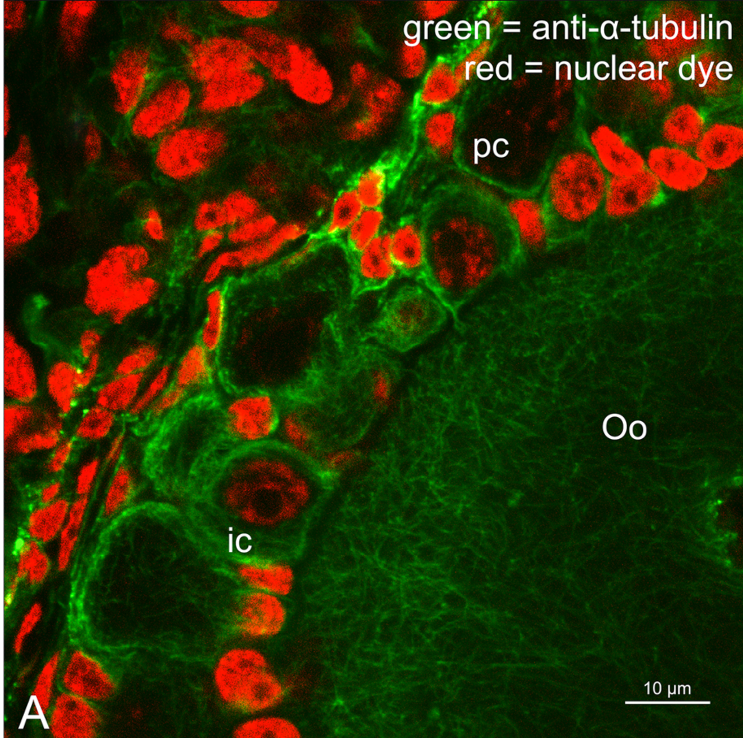
green = anti-α-tubulin
red = nuclear dye
pc
Oo
ic
10 µm
A

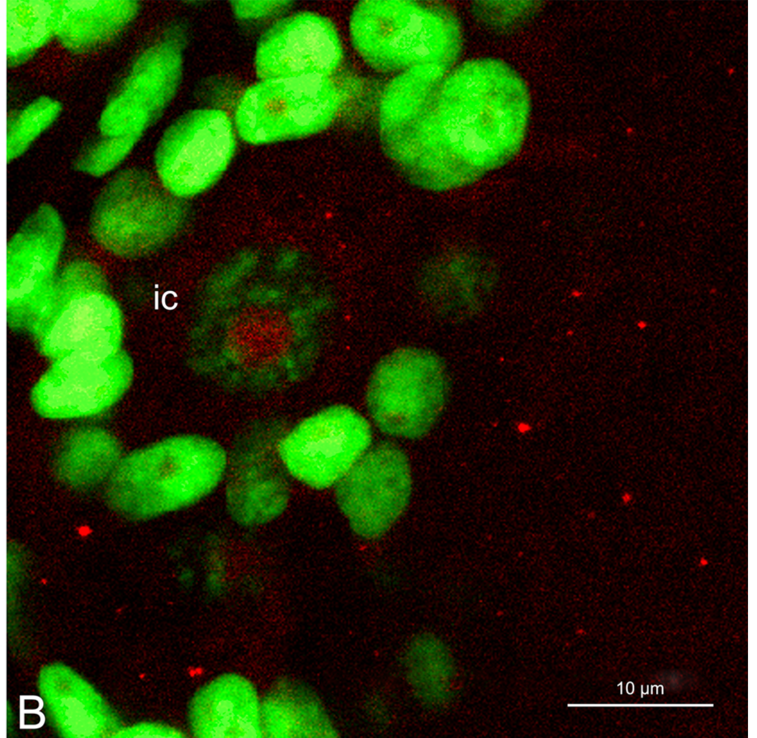
ic
10 µm
B

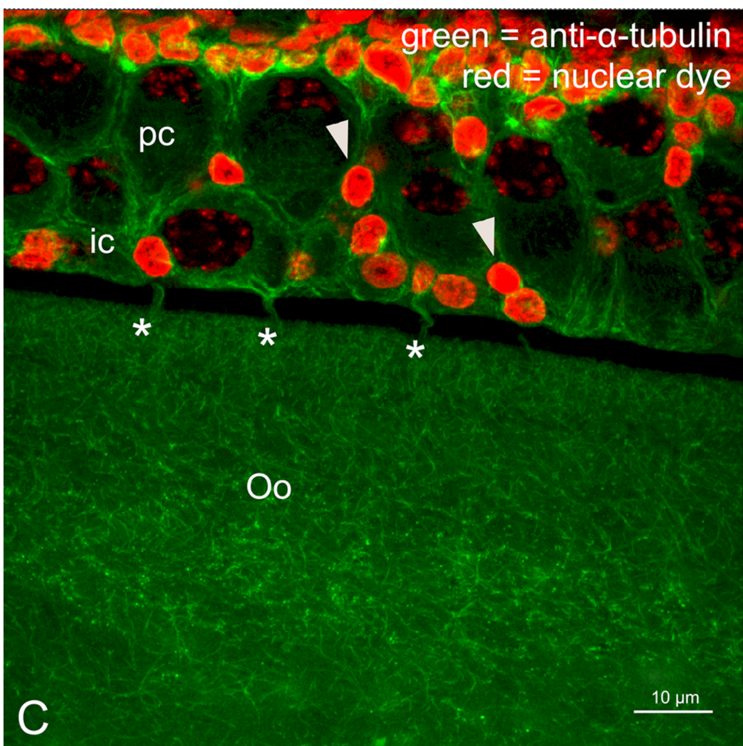
green = anti-α-tubulin
red = nuclear dye
pc
ic
*
*
*
Oo
10 µm
C

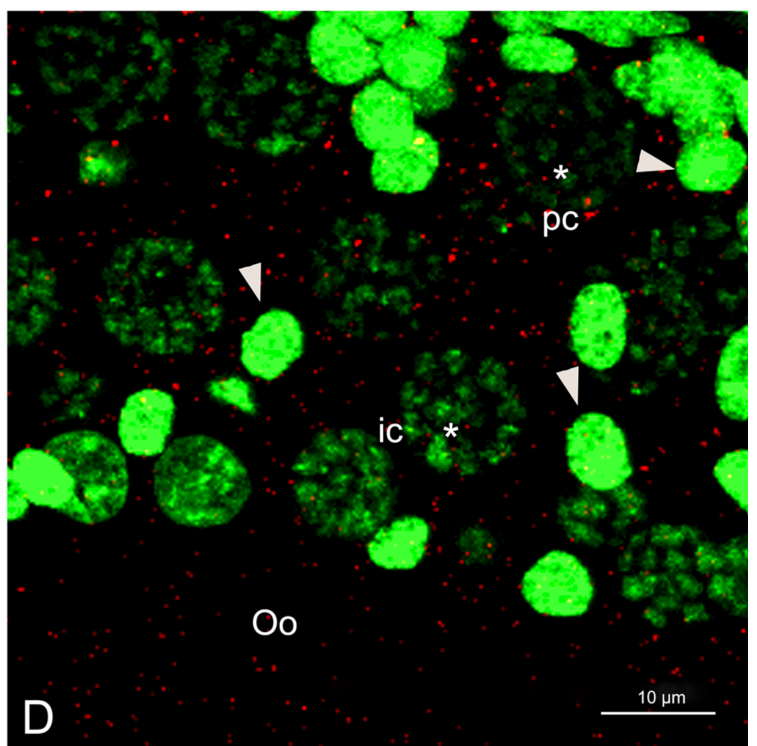
*
pc
ic
*
Oo
10 µm
D

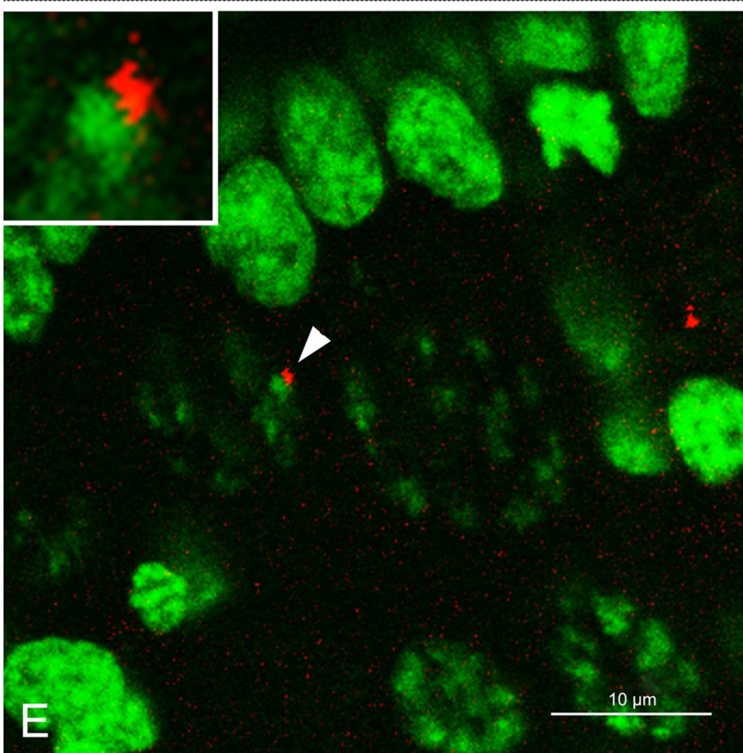
10 µm
E

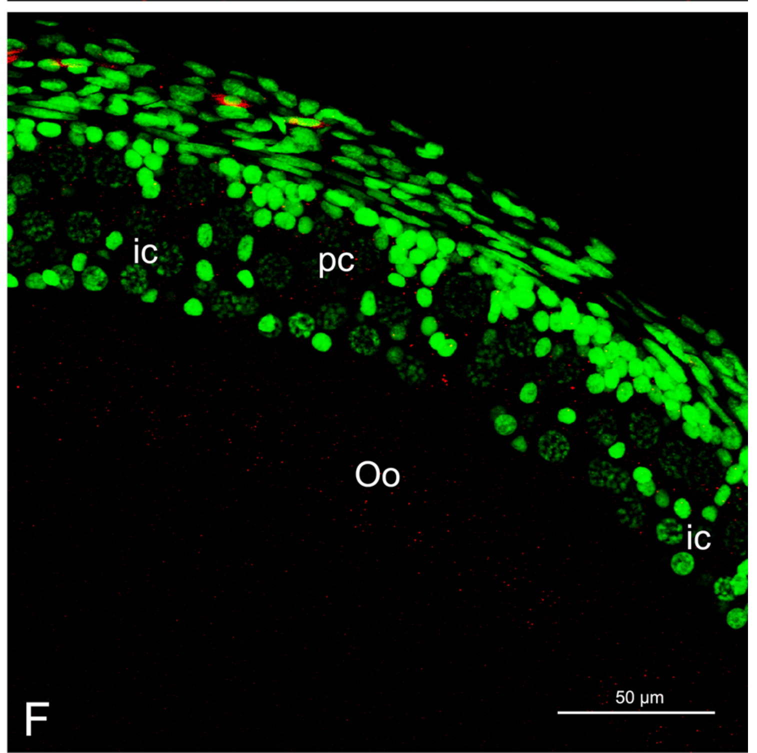
ic
pc
Oo
ic
50 µm
F

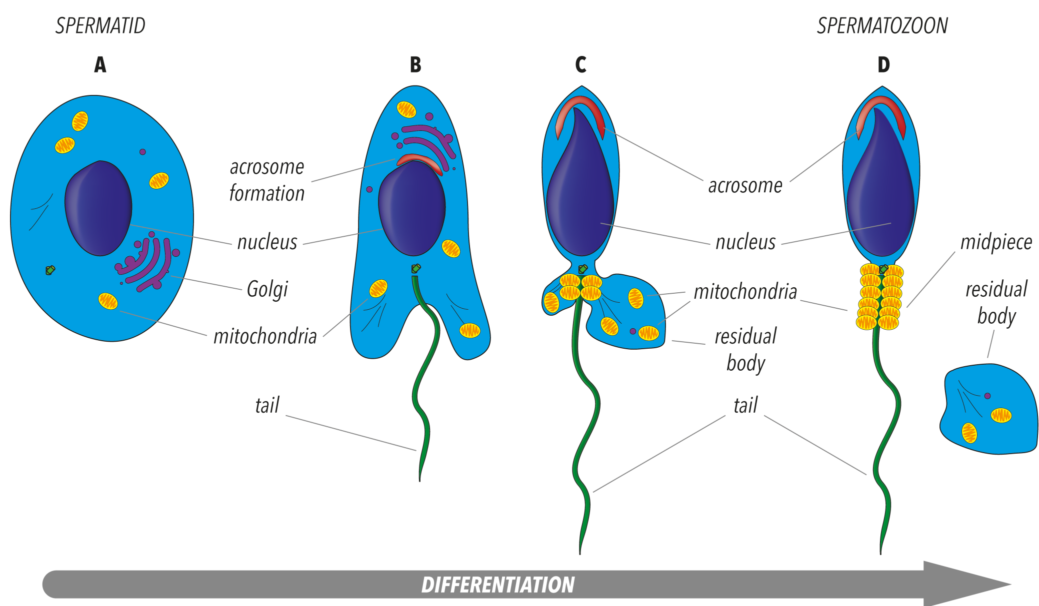
SPERMATID
SPERMATOZOON
A
B
C
D
acrosome formation
nucleus
Golgi
mitochondria
tail
acrosome
nucleus
mitochondria
residual body
tail
midpiece
residual body
DIFFERENTIATION